HYDROXYL TAGGING VELOCIMETRY IN SUPERSONIC FLOW OVER A WALL CAVITY FLAMEHOLDER

BY
MICHAEL DAVID LAHR

MECHANICAL ENGINEERING

HYDROXYL TAGGING VELOCIMETYRY IN SUPERSONIC FLOW OVER A WALL CAVITY FLAMEHOLDER

MICHAEL DAVID LAHR

Thesis under the direction of Professor Robert W. Pitz

Hydroxyl tagging velocimetry (HTV) in supersonic flow over a cavity flameholder is presented in this thesis. HTV is an "unseeded", non-intrusive method to measure gas velocity that produces a hydroxyl tag from water vapor naturally occurring in humid air. These types of gas phase velocity measurements are needed in supersonic flows where probes can easily cause flow disturbances. Typical gas phase velocity measurements are accomplished through laser scattering from particles naturally occurring in the flow or of those inserted in the flow. However, these particles can coat test section windows and exhibit drag biasing, altering the accuracy of the gas phase velocity data.

The ambitions and motivation for this work under direction of Vanderbilt University and the United States Air Force are first presented. An overview of HTV, and the reasons associated with its ideality for supersonic application are also presented. In addition, the alternate velocimetry techniques and their subsequent downfalls to this area are discussed. Hydroxyl tagging velocimetry is demonstrated in Mach 2 flow in the combustor test section of a model scramjet engine at Wright-Patterson Air Force Base.

Instantaneous, single-shot measurements of two-dimensional flow patterns are made in the non-reacting Mach 2 flow with a wall cavity under both low and high backpressure conditions. The single-shot profiles are analyzed to yield mean and root-mean-squared velocity profiles in the Mach 2 non-reacting flow. A description of the post-processing technique for the HTV images is presented and the subsequent results are provided. Finally, hydroxyl tagging velocimetry work that is in progress and that which is planned for the future is discussed.

HYDROXYL TAGGING VELOCIMETYRY IN SUPERSONIC FLOW OVER A WALL CAVITY FLAMEHOLDER

By

Michael David Lahr

Thesis

Submitted to the Faculty of the

Graduate School of Vanderbilt University

in partial fulfillment of the requirements

for the degree of

MASTER OF SCIENCE

in

Mechanical Engineering

December, 2005

Nashville, Tennessee

Approved:

Dr. Robert W. Pitz

Dr. Mark A. Stremler

Dr. Deyu Li

To my parents, Steve and Mary Ann Purkiser

Thank you for all of your love and support.

“The only true wisdom is in knowing you know nothing.”

- Socrates

“All that is gold does not glitter; not all those that wander are lost.”

- J.R.R. Tolkien

ACKNOWLEDGEMENTS

I would first like to thank Dr. Robert Pitz from Vanderbilt University and Dr. Campbell Carter from the Wright-Patterson Air Force Base Research Labs for their superior guidance and encouragement throughout this research. Special appreciation goes out to Zachary Douglas for his work and time spent at the Wright-Patterson AFB. I would also like to acknowledge Shengteng Hu from Vanderbilt University, Joe Wehrmeyer from Arnold Engineering Development Center, and the technicians at the Air Force Research Labs for their continued willingness to aid in any aspect of the hydroxyl tagging velocimetry throughout the course of this work. Finally, I would like to express my gratitude to Manooch Koochesfahani and Chee Lum from Michigan State University for allowing Vanderbilt to use their molecular tagging velocimetry code, in addition to the time and help put forward in analyzing the HTV data.

Financial support was granted through the summer fellowship research program at Wright-Patterson Air Force Base under the Air Force contractor, Universal Technologies Corporation. In addition, financial support was provided by Arnold Engineering Development Center under contract F40600-03-D-0001. Additional funding for the scramjet facility in Research Cell 19 at Wright-Patterson AFB was provided by the Air Force Office of Scientific Research (AFOSR) under the support of J. Tishkoff.

My greatest acknowledgement and show of gratitude goes to my family for their unconditional support and love throughout my studies at Vanderbilt. Without their willingness to provide for me unending opportunities at expense to themselves, none of this would be possible. Thank you, Mom, Dad, Joey, and Bailey.

TABLE OF CONTENTS

LIST OF TABLES

LIST OF FIGURES

CHAPTER I

INTRODUCTION

1.1 Motivation and Goals

Hypersonic flight vehicles and missile systems using air breathing propulsion technology are a vital part of advancing homeland security and space exploration. Fast-strike or fast reconnaissance systems using hypersonic capabilities can greatly aid in the detection and subsequent stop to terrorist threats. In addition, the use of hypersonic air breathing systems instead of costly and heavy on board oxidizers can make space exploration cheaper and easier.

In developing hypersonic capabilities there is a great need for research and experimentation in many fields. Realistic test areas and test conditions are needed to first simulate performance; however, methods for obtaining data in extreme conditions are also desired. In addition, modeling, in particular computational fluid dynamics (CFD) models, can be used as a low cost means of designing robust hypersonic systems. Data sets are needed to validate these CFD models. Of significant importance, are measurements of velocity. In supersonic and hypersonic flows, the high gas velocities make the use of intrusive systems and probes inadequate. Laser-based diagnostic methods provide a means of measuring gas velocity in high temperature, high speed, concentrated flow and can provide complete data sets for modeling and simulation.

The Air Force is developing a Mach 8 hypersonic missile powered by a hydrocarbon-fueled, dual-combustion ramjet. The Arnold Engineering Development

Center facilities in Tullahoma, TN provide an adequate environment for qualification tests. The APTU (Aerodynamic and Propulsion Test Unit) facility is a blowdown facility designed for true temperature aerodynamic, propulsion, and material/structures testing. Using a Marquart SUE burner coupled to the APTU Mach 8 nozzle, a dual-combustion ramjet will be tested in the flow exiting the Mach 8 free jet nozzle. Velocity field measurements are needed to characterize the nozzle and ramjet flow. However, before these tests are conducted, a demonstration was needed of flow tagging in a ramjet facility. This demonstration has been conducted at Wright-Patterson Air Force Base in Dayton, OH. A scramjet combustor test section was used in the supersonic Mach 2 wind tunnel in Research Cell 19 at the Air Force Research Laboratory in the Propulsion Directorate. The hydroxyl tagging velocimetry (HTV) work conducted there is the basis for this thesis.

1.2 Organization

To put this work into a more easily understandable framework, the organization of this thesis is presented. The different laser diagnostic techniques for measuring gas velocity and the subsequent reasons for choosing hydroxyl tagging velocimetry are discussed in Chapter II. Chapter III outlines the details of HTV and presents the past work using this molecular-based velocimetry method. The work and results from Wright-Patterson in 2004 are presented in Chapter IV, while the work and results from 2005 are discussed in Chapter V. Chapter VI details the current work and future aspirations for this technique, and, finally, conclusions on hydroxyl tagging velocimetry are summarized in Chapter VII.

CHAPTER II

LASER DIAGNOSTIC TECHNIQUES FOR MEASURING GAS VELOCITY

2.1 Particle-Based Velocimetry Methods

In supersonic flows, probes can easily produce flow disturbances. In this case, non-intrusive measurements of velocity are needed to accurately describe the velocity field. Typically, non-intrusive gas-phase velocity measurements are made with laser scattering from particles either inserted or naturally available in the flow. A popular technique, particle image velocimetry, consists of illuminating particles in a flow and utilizing a camera to detect the motion of the displaced particles. Other particle-based methods include techniques involving the Doppler shift of light. These include laser Doppler velocimetry, planar Doppler velocimetry, and phase Doppler anemometry. In these techniques, particles in the flow pass through a laser beam. The subsequent light scattered by the particles is Doppler shifted in frequency. The magnitude of the shift is dependent on the propagating direction of the laser as well as the viewing region under investigation. The wavelength, or frequency, of the particles after the shift is recorded by a detector and can be computed into velocity vectors. In comparison to the speed of light, the velocities encountered in Doppler shift techniques are very small. Therefore, the subsequent Doppler shift is also small, which makes this type of method more accurate at higher velocities due to the limited capabilities of high resolution equipment (Adrian 1991 and Drain 1980).

The use of particles in laser velocimetry requires the particles to follow the fluid streamlines of the corresponding unseeded flow. However, this is not always the case. In supersonic flows the particle velocity often differs from the actual gas velocity due to particle drag and a slow response to velocity gradients. Nichols (1985) was able to show that for seeded particles passing through a shock wave, the particle lag can be substantial. On the other hand, Hjelmfelt and Mockros (1966) demonstrated that particles under a high-frequency, oscillating flow field may underestimate the turbulence intensity of the flow. Besides the flow field problems, particles in confined flow can also pose other concerns. Particles can coat test section windows, leading to limited test times or even window abrasion. Rocket tests in the Propulsion Engineering Research Center at The Pennsylvania State University used aluminum oxide (Al_2O_3) particles with a nominal diameter of 0.3 μm to perform Doppler shift measurements. Deposition of the aluminum oxide particles on the windows limited operation and shortened run times. Seeding limitations also impacted the flow rate and locations in the test section available for measurements. Smaller particles can alleviate some of these problems, but particles tend to agglomerate to form larger bodies. Moreover, when using Doppler shift methods, smaller particle size leads to a decrease in the signal intensity in an already limited approach (Santoro 2001).

2.2 Molecular-Based Velocimetry Methods

Another widely used technique, which can negate many problems posed by particle methods, is laser-based molecular velocimetry. Due to the inherent problems associated with particle methods in supersonic conditions, molecular velocimetry is the

technique to be applied to the scramjet combustor at Wright-Patterson Air Force Base. Unlike particle-based methods, laser-based molecular techniques directly measure the gas velocity instead of using the velocity of particles which may or may not follow the fluid streamlines. Like particle methods, molecular velocimetry can either consist of "seeding" the flow with molecules (or atoms) or using those naturally available in the chemical composition of the flow. Doppler-shift methods typically use molecules that are "seeded" to the flow. Many of these Doppler-based molecular velocity methods are based on laser-induced fluorescence of molecules that are added to the flows such as copper (Marinelli et al. 1991), hydroxyl (Allen et al. 1994 and Klavuhn et al. 1994), nitric oxide (Paul et al. 1989), sodium (Zimmermann and Miles 1980), and iodine (McDaniel et al. 1983). Copper atom based laser Doppler measurements of velocity were made successfully by Marinelli et al. at the NASA/JSC 10 MW arc jet facility to demonstrate a technique capable of describing the fundamental parameters associated with arc jet flowfields including velocity and turbulence in the compressible flow. Typically, conventional intrusive probe techniques such as hot-wire anemometry are sufficient to record velocity. However, hot-wire anemometry is limited in compressible flow due to its response to velocity fluctuations. In addition, the probe associated with this method can cause shock waves, distorting the flow. Laser Doppler anemometry (LDA) uses the Doppler-shift of light scattered off particles to determine velocity. This non-intrusive method is sufficient in compressible flow and exceeds the response of most hot-wire approaches. However, these particles do not survive long in extreme high temperature environments and suffer from slip in high velocity flows. Therefore, Doppler fluorescence of the seeded copper atoms was the method chosen (Marinelli et al. 1991).

As mentioned before, hot-wire anemometry and particle-based laser-Doppler anemometry are inapplicable in high temperature, high enthalpy, combusting test environments. The fluctuations and short exposure times leave much room for error. Hydroxyl Doppler-shifted fluorescence imaging of velocity has been demonstrated in reacting supersonic flow. This fluorescence approach again circumvents many of the previous limitations. Moreover, hydroxyl is a reactant available in many hot flow experiments (Allen et al. 1994 and Klavuhn et al. 1994). Another widely used seed molecule is NO. Paul et al. (1989) used pulsed planar laser-induced fluorescence, which is based on Doppler-shift, to obtain velocity components in a Mach 7 underexpanded supersonic jet. A major difference between this work and previous work in this area, is the use of broadband laser excitation, which increases the range of Doppler-shifts that can be measured (Paul et al. 1989). Sodium has also been used, with Zimmermann and Miles (1980) demonstrating Doppler-based velocimetry with the use of this atom in hypersonic helium flow. A tunable dye laser was used to excite sodium vapor for velocity measurements. However, the downside to this application is that sodium seeding requires injection at high temperature. This can perturb the state of the entire flowfield. McDaniel et al. (1983) supplemented this work with a non-perturbing iodine seeding technique in supersonic flow. Iodine can be seeded at room temperature and therefore does not perturb the flowfield. It also has a broad visible absorption spectrum, making the use of several laser sources possible, and provides strong fluorescent signals even in high-density flows (McDaniel et al. 1983). Other Doppler-shift velocity methods are based on Rayleigh scattering from the gas molecules (Seasholtz et al. 1992). Rayleigh scattered light is proportional to gas density and can also be used to obtain temperature if

the pressure is known. The main problem with Rayleigh scattering for diagnostics is that the signal is typically weaker than fluorescence and it is affected by the interference caused by laser scattering from the walls and particles in the flow. This makes Rayleigh scattering signals weak and difficult to obtain (Houwing et al. 2001).

Although there has been success with the use of Doppler-based molecular velocimetry methods that use, the addition of chemical species is often impractical in test facilities. Seeding a large facility can become very expensive. Moreover, seeding may pose a risk for high levels of toxicity and corrosive behavior, and many of these seeded molecules exhibit thermal decomposition at higher temperatures. Also, in Doppler-shift methods the optical geometry of the laser and the observer define the velocity component that is measured, and this feature can be limiting (Houwing et al. 2001). Many laser-induced fluorescence methods that make use of the Doppler-shift can only be used to measure the component of the velocity in the direction of propagation of the laser sheet.

Another molecular-based laser diagnostic option is molecular tagging. In a variety of molecular tagging methods, the molecules or atoms naturally occurring in the flow are used as the source of fluorescence. However, many molecular tagging methods use a gas seed. Molecular tagging techniques yield the gas velocity by time of flight; the molecules in the gas flow are tagged or marked with a laser, and the movement of the tag gives the velocity. Once a laser line or grid is tagged, the grid will move with the flow. There is no particle drag or non-uniformity issues associated with molecular velocimetry. The movement of the tagged regions is imaged by a method dictated by the photochemistry of the tagged molecules. The displacement of the tagged grid over a fixed time period yields the velocity. This time-of-flight measurement of velocity can be

easily implemented because it does not require the complex calibrations or corrections necessary in the Doppler shift method. As already mentioned, some molecular tagging methods, similar to Doppler-based molecular velocity methods, use a gas seed. A gas molecule (or atom) is added to the flow and the molecule is tagged with a laser beam. The molecule can, for example, be electronically excited, photodissociated, or vibrationally excited. Researchers have used a variety of molecular tags in this technique including biacetyl (Hiller et al. 1984; Stier and Koochesfahani 1999), acetone (Lempert et al. 2002), nitric oxide (Houwing et al. 2001; Danehy et al. 2003), nitrogen dioxide (Orlemann et al. 1999), tert-butyl nitrite (Krüger and Grünefeld 1999), sodium (Barker et al. 1995), and strontium (Rubinzstein-Dunlop et al. 2001). Again, seeding a flow with molecules or atoms is often undesirable due to a variety of reasons (expense, seeding toxicity, corrosive behavior, thermal decomposition, etc.).

Biacetyl seeding was demonstrated by Hiller et al. (1984) and Stier and Koochesfahani (1999) in gas flows for instantaneous, multipoint velocimetry. However, the phosphorescence of the non-toxic tracer is easily quenched by oxygen, preventing application to air flows. Typically, a nitrogen chamber has to be used to conduct these measurements. A major upside to biacetyl tagging is the need for only one laser. The biacetyl is excited by one laser with its displacement and then imaged. This can greatly reduce the cost and setup time for an experiment. Acetone has also been used as a molecular tag and was demonstrated in sonic and supersonic jets produced by a 1-mm exit diameter nozzle. Acetone photophysics are similar in may respects to biacetyl, except that it is excited in the wavelength range of approximately 230-240 nm instead of at around 270 nm or 420 nm in the case of biacetyl. Acetone does, however, have a short

lifetime, which decreases with an increase in pressure to less than 50 ns at 24 mbar (Lempert et al. 2002). Danehy et al. (2002) used nitric oxide molecules to measure velocity profiles in a Mach 8.5 laminar, hypersonic boundary layer in the Australian National University's T2 free-piston shock tunnel. They also demonstrated this method in the separated flow region forward of a blunt fin attached to a flat plate in a Mach 7.4 flow produced by the Australian National University's T3 free-piston shock tunnel. There are advantages and disadvantages to this type of molecule. Nitric oxide tagging, like biacetyl tagging, requires only one laser. Also, this method requires much lower pulse energy (~ 1 mJ) compared to many other flow-tagging methods. However, the major disadvantage of nitric oxide tagging is the limitation set on the flow velocity by the laser sheet width and fluorescence lifetime. This limitation restricts the application to high-velocity, low collisional quenching (i.e. low pressure) flow environments (Danehy et al. 2002). Seeding a flow with NO_2 has also been used to characterize the small-scale behavior of turbulent air flows. Orlemann et al. (1999) demonstrated this technique by writing a spatial line of NO into an air flow seeded with NO_2 using an XeCl excimer laser (308 nm). Another molecule that can be seeded in a flow in order to use NO as a tag is tert-butyl nitrite. In this technique, a broadband ArF excimer (193 nm) laser dissociates tert-butyl nitrite ($(CH_3)_3CONO$) to form $(CH_3)_3CO$ and NO. When using tert-butyl nitrite as a seed instead of NO_2 to form an NO tag, much less laser energy is needed for generating tag lines. Therefore, a large number of lines can be created, whereas a single tag line was used in work conducted by Orlemann et al. (1999). Barker et al. (1995) have used sodium in an air-acetylene flame to obtain velocity measurements. Using a combination of laser enhanced ionization (LEI) and laser induced fluorescence, flame

velocities were determined with an accuracy of better than 10 %. LEI is an analytical technique that allows for a particular species (in this case, sodium ions) to persist for milliseconds in a flow and is used to tag a region within a gaseous environment. Another flow tagging method utilizing ionisation is demonstrated by Rubinsztein-Dunlop et al. (2001). Strontium is first ionised and then fluoresced to give two dimensional velocity images. Air-acetylene flames were investigated, yielding results sufficient to show that strontium flow tagging can be used for velocity measurements. However, the produced strontium ions have a short decay time (μs), limiting the time delays that can be used for measurements. Therefore, this method, in its current stage, is better suited for supersonic and hypersonic flows where time delays should yield a sufficiently large displacement of the tagged region to determine precise velocities.

There are also unseeded tagging methods, in which tags are created from molecules naturally occurring in air. Examples of molecular tags produced from air are N_2^+ ion (Ress et al. 1995), ozone (Pitz et al. 1996; Ribarov et al. 1999; Pitz et al. 2000), hydroxyl (Pitz et al. 2000; Boedeker 1989; Davidson et al. 1991; Wehrmeyer et al. 1999; Ribarov et al. 2002; Ribarov et al. 2004), nitric oxide (Dam et al. 2001; Sijtsema et al. 2002; van der Laan et al. 2003), and vibrationally excited oxygen (Miles and Lempert 1997 ; Noullez et al. 1997). Many of these methods used nonlinear laser excitation (Miles and Lempert 1997; Ress et al. 1995; Boedeker 1989; Dam et al. 2001; Sijtsema et al. 2002; van der Laan et al. 2003; and Noullez et al. 1997) to produce these tags from air. In this case, the tag is produced only in a small region near the laser focus.

Ress et al. (1995) have demonstrated the use of N_2^+ tracers as an unseeded molecular velocimetry tag. The ions are formed by a multiphoton interaction with the

third harmonic of a Nd:YAG laser and are detected by a negatively biased ion probe in the flow. This method was used to investigate velocities in a low-speed freejet and in the flame of a propane-air torch. N_2^+ is much more effective as a tag in higher speed flows due to the lifetime of the ion. However, the probe poses a problem in areas where non-intrusive data is needed. Dam et al. (2000) and Sijtsema et al. (2002) have investigated nitric oxide tagging in slow laminar dry-air flow and on flow generated by a pulsed valve. An advantage of tagging NO is its long lifetime and good visualization. Moreover, since the tagging scheme requires only N_2 and O_2 molecules, it can be used in ambient air or any other flow system without the need for molecular seeding. Nitric oxide tagging has also been demonstrated by van der Laan et al. (2003) in the base flow behind a wedge in the supersonic flow field of a small wind tunnel. Their technique entitled air photolysis and recombination tracking (APART) was applied in a small Mach 3 wind tunnel to measure the velocity profile behind the wedge as a means of comparison to simulated data. Noullez et al. (1997) have used the Raman-exciting of oxygen molecules and subsequent interrogation by laser-induced electronic fluorescence to write lines in turbulent round jets in air. This method, called RELIEF, was used to obtain non-intrusive measurements of the streamwise velocity in the jets. The major advantage of RELIEF is that it can measure transverse velocity increments over distances at least one order of magnitude smaller than can be measured with typical intrusive techniques. However, the signal-to-noise ratio, or brightness of the lines, still needs to be improved.

Ozone tagging velocimetry is a non-intrusive, unseeded, time-of-flight velocity measurement technique. An excimer laser, preferably operating narrowband at 193 nm, creates an O_3 line via ultra violet absorption. A 248-nm excimer laser then

photodissociates the O_3 and fluoresces the vibrationally excited O_2 product, revealing the tag line displacement. This technique can write long tag lines (~40 mm) due to the single-photon processes of both the write and read steps being insensitive to beam focus. However, ozone tagging velocimetry is a technique better suited for low-temperature gas-flow velocity measurements even though tracking both low and high velocities is possible (Pitz et al. 1996; Ribarov et al. 1999; Pitz et al. 2000). Ozone tagging velocimetry's counterpart, hydroxyl tagging velocimetry, is more suited for high-temperature flows.

In this work conducted at Wright-Patterson Air Force Base, the hydroxyl based molecular tagging method was used. Hydroxyl tagging velocimetry is a linear method (Wehrmeyer et al. 1999; Ribarov et al. 2002; Ribarov et al. 2004) in which an ArF laser, operating at 193 nm wavelength, photodissociates water in a humid flow. In this single-photon process, photodissociation of vibrationally excited H_2O creates lines of OH at a concentration higher than the ambient OH. The OH grid moves for a known period of time and is recorded with laser-induced fluorescence. Hydroxyl is an optimal tag for this supersonic application as OH is formed immediately by the pulsed laser through H2O photodissociation and OH has an adequate lifetime in the supersonic flow. Also, the use of hydroxyl allows for long lines to be written in a hot flow associated with a scramjet, creating more flexibility and accessibility in the test area setup. Hydroxyl tagging velocimetry (HTV) avoids the problems associated with particle-based methods and molecular-methods in which the flow must be seeded.

Non-intrusive velocity data is needed in flows relevant to scramjet combustion. In scramjets, wall cavities are commonly used to stabilize the core-flow flame without excessive drag penalty. They also provide a recirculation region with sufficient residence

time for self-sustaining reaction and core-flow mass exchange. At Wright-Patterson Air Force Base, an optically accessible supersonic flow facility has been developed to study cavity-stabilized supersonic reacting flows. Velocity data from this study can be used as a comparison or parameter for advanced CFD models. In this work, the HTV method is applied to a Mach 2 flow with a wall cavity flame holder to obtain instantaneous two-dimensional velocity images, mean velocity profiles, and rms velocity profiles. Velocity measurements are made by using HTV in the freestream and within the cavity of the Mach 2 cavity-piloted combustor.

CHAPTER III

HYDROXYL TAGGING VELOCIMETRY OVERVIEW

3.1 Introduction

Hydroxyl Tagging Velocimetry (HTV) produces an OH molecular tag through the single photon photodissociation of H_2O molecules in a moist flow that persists in air or hot combustion products. A conceptual drawing of the HTV process is shown in Fig. 3-1. An ArF excimer laser beam (~ 193 nm) is focused into the desired section of a humid flow in which the laser photon dissociates H_2O in its highly repulsive $A^{\sim 1}B_1$ excited state via a broad, structureless absorption continuum (Engel et al. 1987 and Okabe 1978) to "write" a grid of OH lines:

$$H_2O(X^1A_1) + h\nu_{\lambda=193nm} \rightarrow H_2O(A^{\sim 1}B_1) \rightarrow OH(X^2\Pi) + H(^2S) \qquad (2\text{-}1)$$

A light sheet from a second laser excites the OH to fluoresce in the "read step" by invoking the $A^2\Sigma^+ \leftarrow X^2\Pi_i$ OH electronic transition by absorption of a light photon:

$$OH(X^2\Pi_i) + h\nu_{\lambda=248,268,282,or\,308nm} \rightarrow OH(A^2\Sigma^+) \qquad (2\text{-}2)$$

Within the $A^2\Sigma^+ \leftarrow X^2\Pi_i$ electronic transition, the OH signal can be measured by pumping the $(3 \leftarrow 0)$, $(2 \leftarrow 0)$, $(1 \leftarrow 0)$, or $(0 \leftarrow 0)$ vibrational transitions of OH using

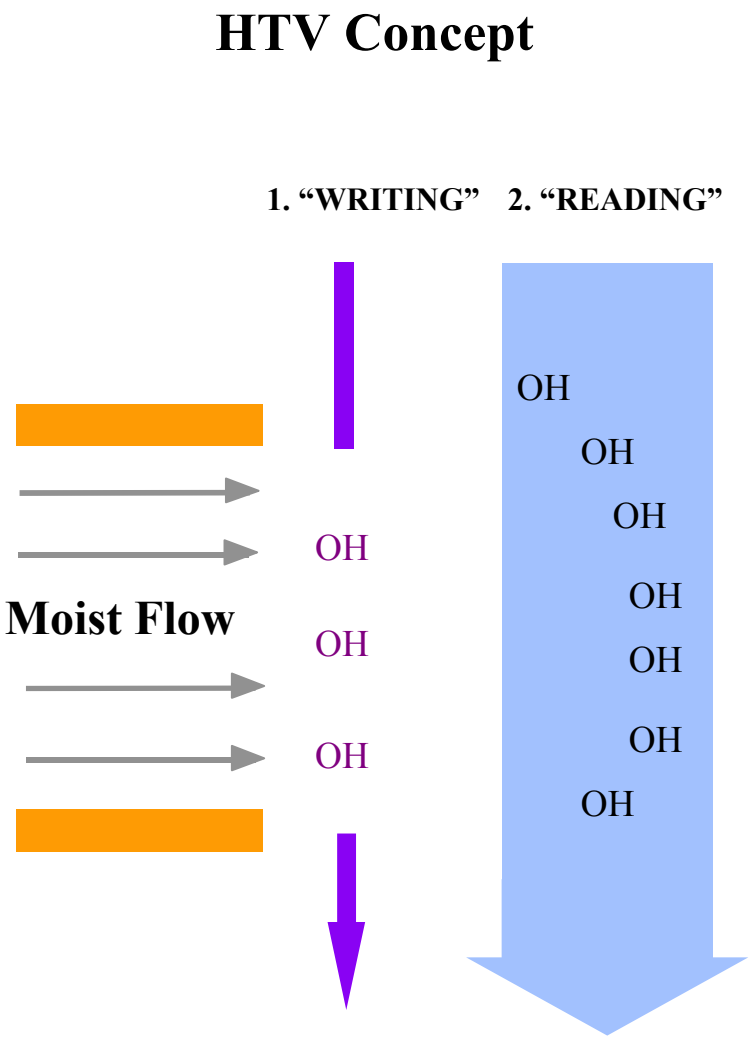

Fig. 3-1. Hydroxyl Tagging Velocimetry (HTV) conceptual schematic.

lasers at 248, 268, 282, or 308 nm. The fluorescence of OH at a specific wavelength is recorded by a CCD camera. Un-delayed and delayed images of OH fluorescence must be recorded to determine the velocity field (Ribarov 2002).

3.2 Past HTV Work

Hydroxyl tagging velocimetry was developed at Vanderbilt University and can be applied to a variety of test configurations and conditions. Initially, hydroxyl tagging was primarily utilized in high temperature diffusion flame flow (Wehrmeyer et al. 1999 and Pitz et al. 2000). Ribarov et al. (2002) then demonstrated HTV in low-temperature (300 K) ambient air flowfields by replacing the KrF "read" laser with a frequency doubled Nd: YAG pumped dye laser to improve upon the weak absorption of ground vibration state H_2O at low temperature. Then Ribarov et al. (2004) implemented the first micro-lens optical system to this procedure, producing a 7 x 7 multi-line optical grid in reacting and nonreacting experimental flows.

Wehrmeyer et al. (1999) demonstrated HTV in a turbulent H_2/N_2-air diffusion flame created by a nozzle 1.8 mm in diameter issuing N_2-diluted H_2 into quiescent air. In this subsonic flow, a 50 μs write-read delay was implemented yielding a measured velocity of approximately 22 m/s. This velocity has an uncertainty of 14% for the test conditions. This uncertainty is partially due to the low velocity of the flow and would decrease in high-velocity combustion flow. Pitz et al. (2000) also made HTV measurements in a lean H_2-air flame ($\phi = 0.41$, 1450 K, 135 slpm total flowrate). The flame was produced by a 12.5 mm diameter 'Hencken' burner, which is a matrix of separate fuel and air tubes that form an array of small diffusion flames that quickly

combine into a uniform stream of adiabatic combustion products. The data yielded a velocity of 75 m/s. A problem associated with HTV in low velocity flows is spreading of the OH tag line from OH and H molecular diffusion. Again, in high speed flows, the time between the writing and reading of the grid can be greatly reduced and will limit the diffusional broadening of lines in the grid.

Ribarov et al. (2002) introduced the use of a pulsed frequency-doubled dye laser to replace the KrF excimer "read" laser that could only access a weak OH transition. The doubled dye laser at 308 nm can access the strong $Q_1(1)$ line in the $(0 \leftarrow 0)$ vibrational band of the $A^2\Sigma^+ \leftarrow X^2\Pi_i$ transition of OH, compensating for the relatively weak 193 nm absorption of room-temperature H_2O. HTV measurements could then be demonstrated in low-temperature and high-temperature flow fields. In this case, tagging measurements were made in an air jet created by a small Hencken burner nozzle. A 3 x 4 grid of tag lines was fluoresced at 308 nm by the doubled dye laser using a 30 μs delay. The measured velocity was 35.3 m/s, which was close to the theoretically expected value for the average jet exit velocity of ~ 28 m/s. The uncertainty was ~ 12 %. An image of a flow field with a larger vector representation was desired after years of HTV experiments. Ribarov et al. (2004) then began using a compact micro-lens optical system to produce a 7 x 7 multi-line optical grid with at least 49 resolvable velocity vectors. The experimental setup for this configuration is shown in Fig. 3-2. HTV measurements were taken in an air jet flowing from the inner nozzle of a small Hencken burner and from an H_2-air flame from a Hecken multi-element diffusion flame burner. Fig. 3-3 is an example of an analyzed HTV image in the H_2-air flame (~ 10 m/s). This setup was the basis for

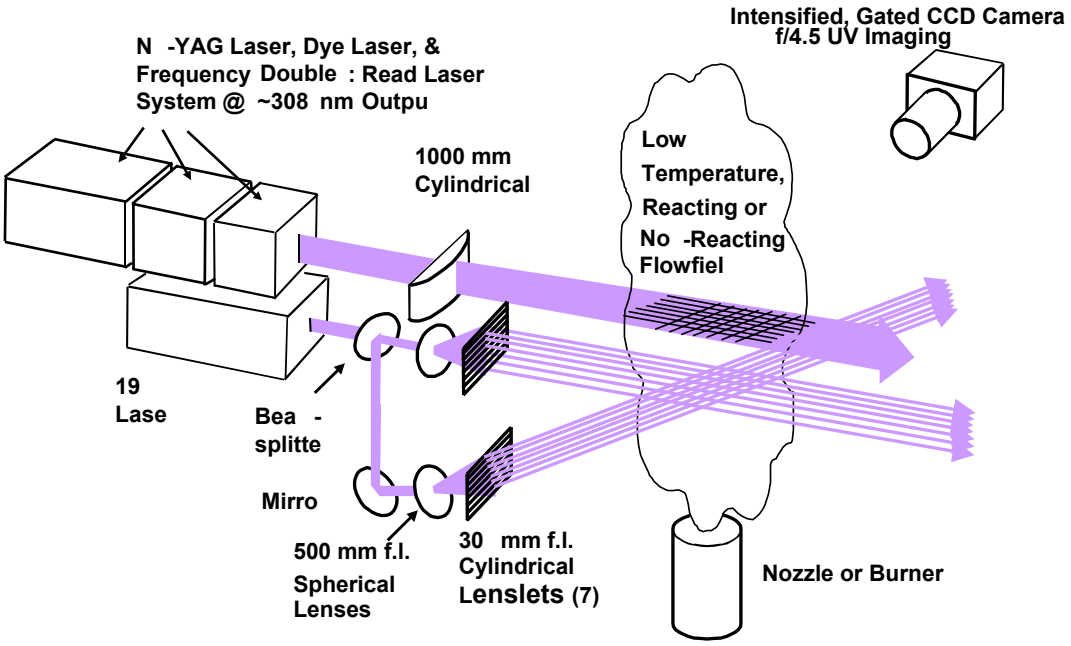

Fig. 3-2. Experimental setup with micro-lens optical system (Ribarov et al. 2004).

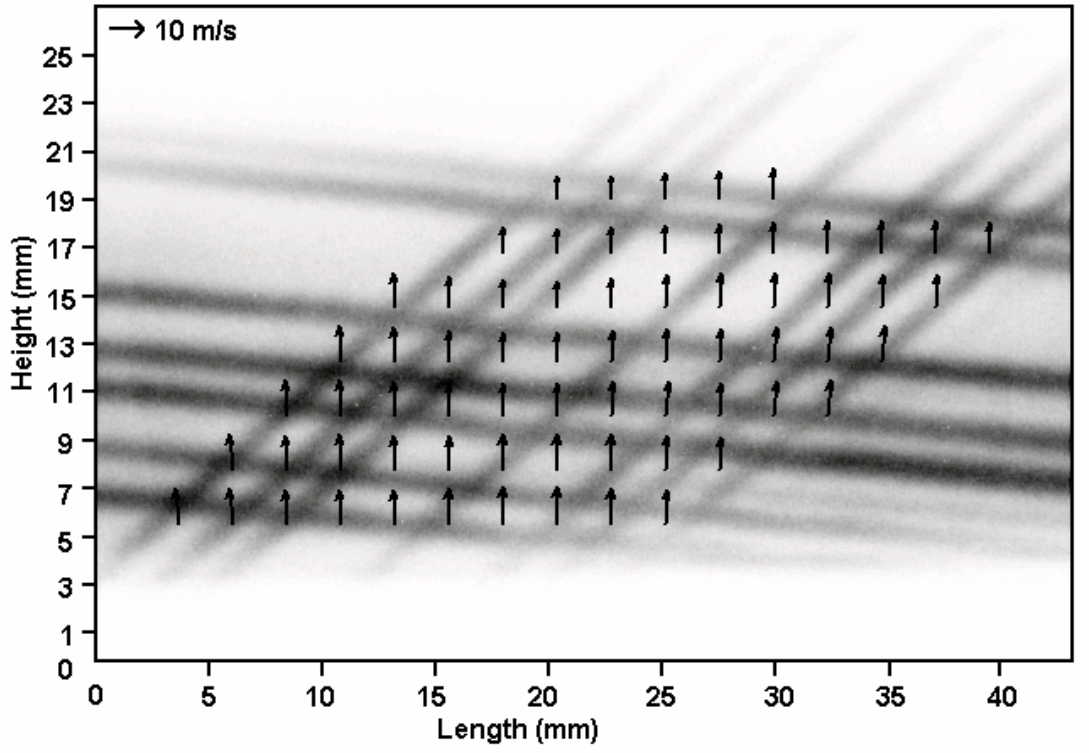

Fig. 3-3. Analysis of HTV image to yield velocity field data using the new optical setup (Ribarov et al. 2004).

the configuration at Wright-Patterson Air Force Base. The same micro-lens optical system was used in the experiments in 2004.

Hydroxyl tagging velocimetry lends itself to supersonic and hypersonic flow as can be seen from previous work. Diffusional broadening of lines in the OH grid and the subsequent uncertainty associated with the measurements is greatly reduced by grid displacement in a small amount of time. With the added benefits of long OH lines and the inherent properties of a molecular tagging method, this technique was chosen as an excellent fit for the scramjet facilities at Wright-Patterson Air Force Base.

CHAPTER IV

HYDROXYL TAGGING VELOCIMETRY AT WRIGHT-PATTERSON AIR FORCE BASE (2004)

4.1 Supersonic Flow Facility

The hydroxyl tagging velocimetry experiments were conducted at the supersonic flow facility in Research Cell 19 at the Air Force Research Laboratory, in the Propulsion Directorate at Wright-Patterson Air Force Base. Fig. 4-1 shows the wind tunnel set up for the research facility. This facility is designed to allow studies of the basic mechanisms governing the mixing and combustion processes within realistic supersonic combustor geometries. An emphasis is placed on using non-intrusive diagnostic techniques to conduct the tests. The facility is capable of variable Mach number, continuous flow operation under a multitude of flow conditions. The test section (5 x 6 in.) was made optically accessible with three fused silica windows to allow visualization of all three orthogonal flow planes. A uniform, two-dimensional, Mach 1.98 stream is present at the entrance to the test section with the flow symmetric about the transverse and spanwise centerlines. The air supply to the wind tunnel consists of a series of compressors and a gas-fired heat exchanger to produce high-pressure/high-temperature air. Desired stagnation conditions can be achieved with the combination of a hot line capable of supplying 17 lbm/s of 750-psig air at 1660^{o}R and a cold line capable of supplying 17 lbm/s of 750-psig air at ambient temperature. These two merge at a mixing station, and an insulated expansion loop transports the mixed air to a supply manifold

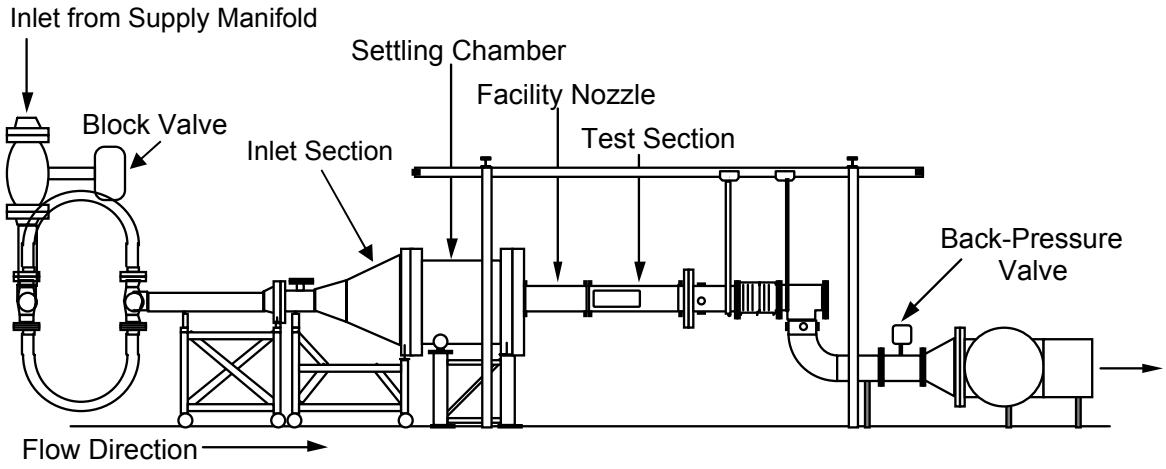

Fig. 4-1. Facility schematic of the supersonic combustion tunnel in Research Cell 19 (Gruber and Nejad 1995).

with five branches (three branches supply air to the clean room, while the other two exit out through the roof) (Gruber and Nejad 1995).

The combustion wind tunnel consists of five major parts: 1) inlet section, 2) settling chamber, 3) nozzle section, 4) test section, and 5) diffuser and flow exit. Four flexible stainless steel hoses connect the right and left manifolds and allow for thermal growth in the upstream direction as the air comes from the supply manifold. The inlet section transports air to the settling chamber. A rearward-facing perforated cone is housed within the expansion section to distribute the flow as it enters the 24-in. settling chamber. The chamber is designed to withstand 400 psig at 1660^{o}R, while producing up to 50 ft/s of air over the desired conditions prior to acceleration by the supersonic nozzle. The settling chamber uses an array of mesh screens and a section of honeycomb to condition the flow. A transition region is housed at the downstream end of the chamber to allow for the nozzle geometry. The constant area test section follows the nozzle. The three fused silica windows (Suprasil with good transmission at 193 nm) on the test section allow for optical access and non-intrusive diagnostic techniques. The back pressure valve allows for shock creation in the test section to simulate the pressure rise due to actual combustion. Finally, the exit air leaves through a spray-cooled diffuser, which cools the gases before leaving the building (Gruber and Nejad 1995).

The tunnel, past the nozzle, has a constant-area isolator section upstream of a flame holder cavity with a cross section of 51 mm high by 153 mm wide. A side view of the isolator and test section regions can be seen in Fig. 4-2. Downstream of the isolator, into the test section, the bottom wall diverges at an angle of 2.5^{o}. A cavity to provide a

flame pilot forms the bottom surface of the tunnel. Fig. 4-3 shows a schematic of the cavity (the flow is now left to right). It is 17 mm deep and 66 mm long. A shear layer forms at the edge of the first step in the cavity, and the recirculation zone is produced by the cavity.

4.2 Experimental System

The HTV measurements were taken in the flame holder cavity of the combustor test section. A schematic of the HTV system is shown in Fig. 4-4. Mach 2 air entered the test section with the air flowrate at about 1.4 kg/s. A Lambda Physik Compex 150T ArF excimer laser was used to produce a 193 nm laser beam. The ArF excimer laser beam (20 mm high by 10 mm wide, 120 mJ/pulse, broadband, 1 nm bandwidth) was split into two beams by a beam splitter. Each of the laser beams was sent through grid-forming optics that produce two sets of seven beams each. The grid optics shown in Fig. 4-5 consist of two major components placed very close together because of their focal lengths: a 300 mm focal length cylindrical lens (25 mm x 40 mm) and a stack of 300 mm cylindrical lenses (20 mm wide by 3 mm high). The beam diameter was about 0.3 mm in the measurement zone. The sets of beams produce 49 crossing points in the measurement zone; however, because of the viewing area of the camera used, only around 28 crossing points are viewable. The energies for the two sets of beams before transmission into the tunnel were measured at 20 mJ on the 2.3 m beam path (left grid) and 10 mJ on the 3.0 m beam path (right grid). With the ArF excimer laser operating broadband instead of narrowband, much of the beam was absorbed by O_2 (about 85%) before the beams crossed in the measurement zone: in principle, the laser can be tuned to avoid O_2

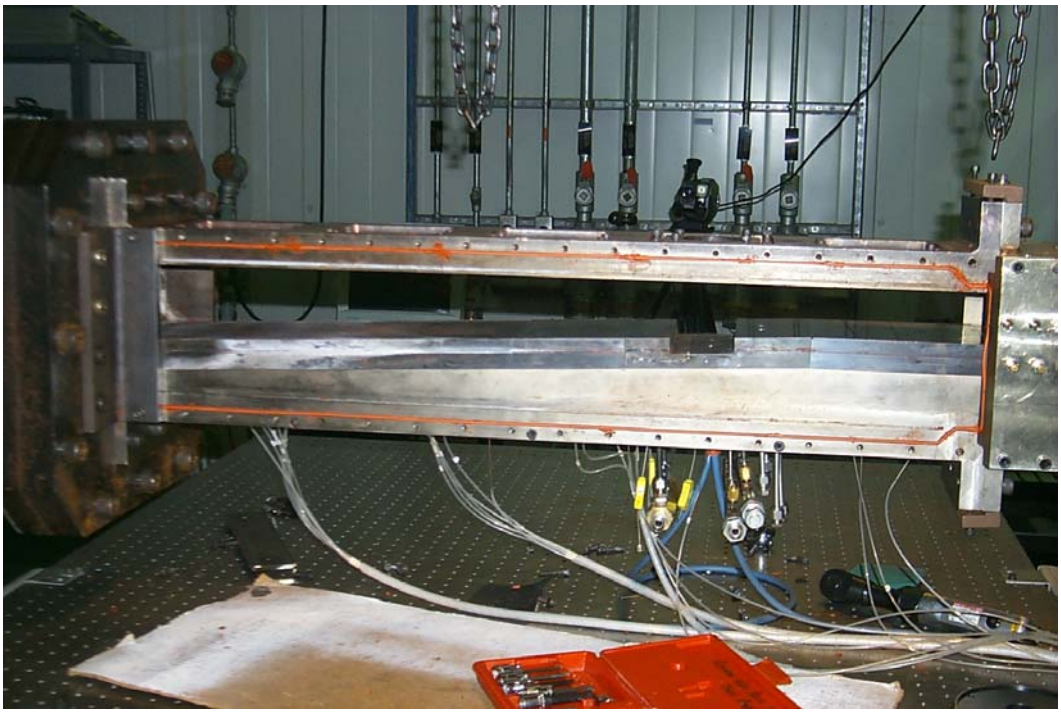

Fig. 4-2. Side view of isolator and test section region (flow is from right to left).

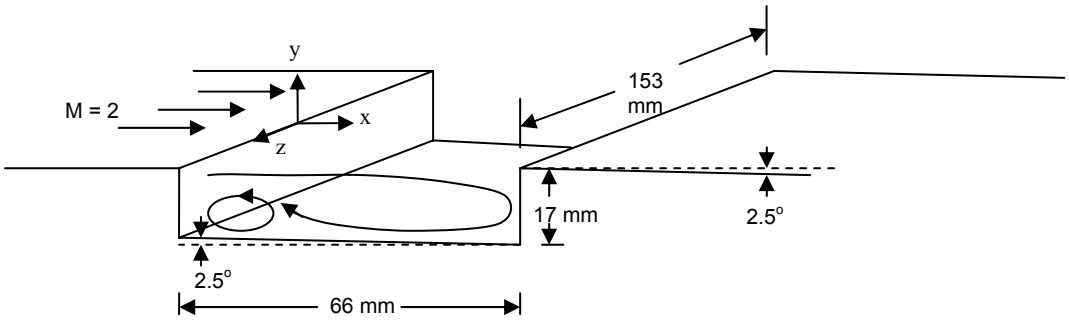

Fig. 4-3. Mach 2 cavity piloted flow.

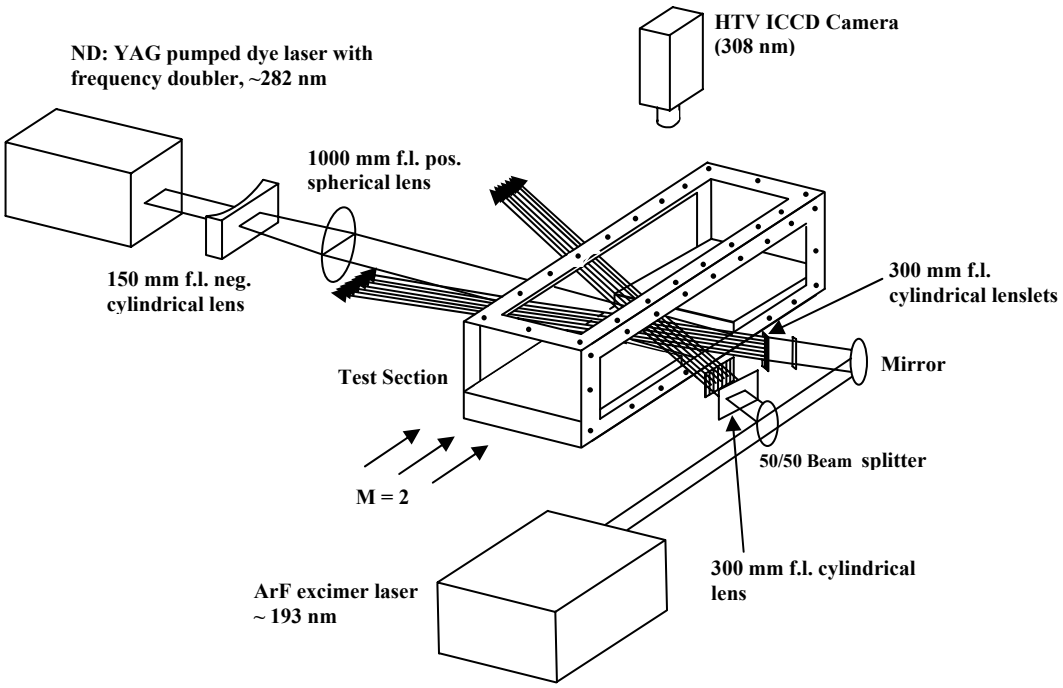

Fig. 4-4. Schematic of the HTV experimental system (2004).

Fig. 4-5. Grid optics setup (300 mm focal length cylindrical lens in front of a stack of seven 300 mm cyldindrical lenses).

transitions, thereby improving beam transmission to the tunnel. This increase in energy can improve grid imaging and improve the postprocessing by increasing the signal-to-noise ratio.

The 7 x 7 grid of ArF-generated "lines" of OH was imaged by laser-induced fluorescence of OH using the $Q_1(1)$ transition of the $A^2\Sigma^+$ ($v' = 1$) $\leftarrow$ $X^2\Pi_i$ ($v'' = 0$) band at 282 nm. A Spectra Physics Model GRC 170 Nd:YAG laser (injection seeded) pumped a Lumonics HD-300 Hyperdye dye laser. The output of the dye laser was doubled by an Inrad Autotracker II to produce about 20 mJ/pulse of 282 nm laser radiation. A small portion of the 282 nm beam was split off and directed over a small flame and then to a photodiode. Signals from the photodiode and a photomultiplier tube—recording the OH laser-induced fluorescence from the flame—were displayed on an oscilloscope to ensure proper operation of the dye laser and good overlap with the OH transition. Timing of the lasers and camera was accomplished with a Quantum Composer (model 9318E) pulse generator. Random (shot-to-shot) timing error between the lasers was about ±20 ns or about ±1% of the typical 2 μs timing separation.

The OH-probe laser beam was expanded by a negative cylindrical lens (focal length = -150 mm) and focused by a 1000 mm focal length spherical lens to form a sheet. To improve the signal strength, the laser sheet was retro-reflected through the tunnel with a delay of about 5 ns. Both this sheet and the 193 nm grid were rotated to be parallel to the tunnel bottom floor (2.5º off the horizontal plane).

Fluorescence from the created OH was recorded using a PIMAX "Superblue" intensified CCD camera, which was fitted with a 45-mm f/1.8 UV lens (Cerco). Schott glass filters (WG-295 or 305 and UG-11) were employed to block background scattering

and fluorescence (from tunnel surfaces). Typically, the 512 x 512 pixel array of the PIMAX camera was binned 2 x 2 to improve the signal strength. The field of view was 40 mm square, and the camera looked down on the cavity through the tunnel top window (also made of Suprasil). Each 2x2 binned pixel imaged a 156 μm x 156 μm region of the flowfield. The region probed was roughly in the spanwise center of the flowfield and either over or within the cavity.

Focusing optics (for both laser systems) and the ICCD camera were mounted on a three-dimensional traversing table located beneath the tunnel as is shown in Fig. 4-6; the lasers, however, were not mounted on this table. The optics between the lasers and traversing table were thus arranged to allow the laser grid and sheet height location to be varied and thus the shear layer and cavity to be probed.

With stagnant room air in the tunnel at ambient pressure, the ArF excimer laser was pulsed to create the OH grid that was subsequently excited by the OH-probe laser sheet after a short delay (~0.2 μsec). The laser-induced fluorescence (LIF) signal was recorded by the ICCD camera and the OH probe laser wavelength was scanned over about 0.7 nm. The resultant laser excitation scan is shown in Fig. 4-7. The measured spectrum was compared to a simulated spectrum calculated by LIFbase (ver. 2) (Luque and Crosley 1999). The measured and calculated line positions match very well. At room temperature (295K), the strongest line is the combined $Q_1(1) + R_2(3)$ peak in the OH A-X (1,0) band. Thus the OH probe laser was tuned to this line for the maximum signal. It is worth noting that transition saturation effects distort the spectrum, thus preventing the spectrum from being adequately fit by a simulated spectra.

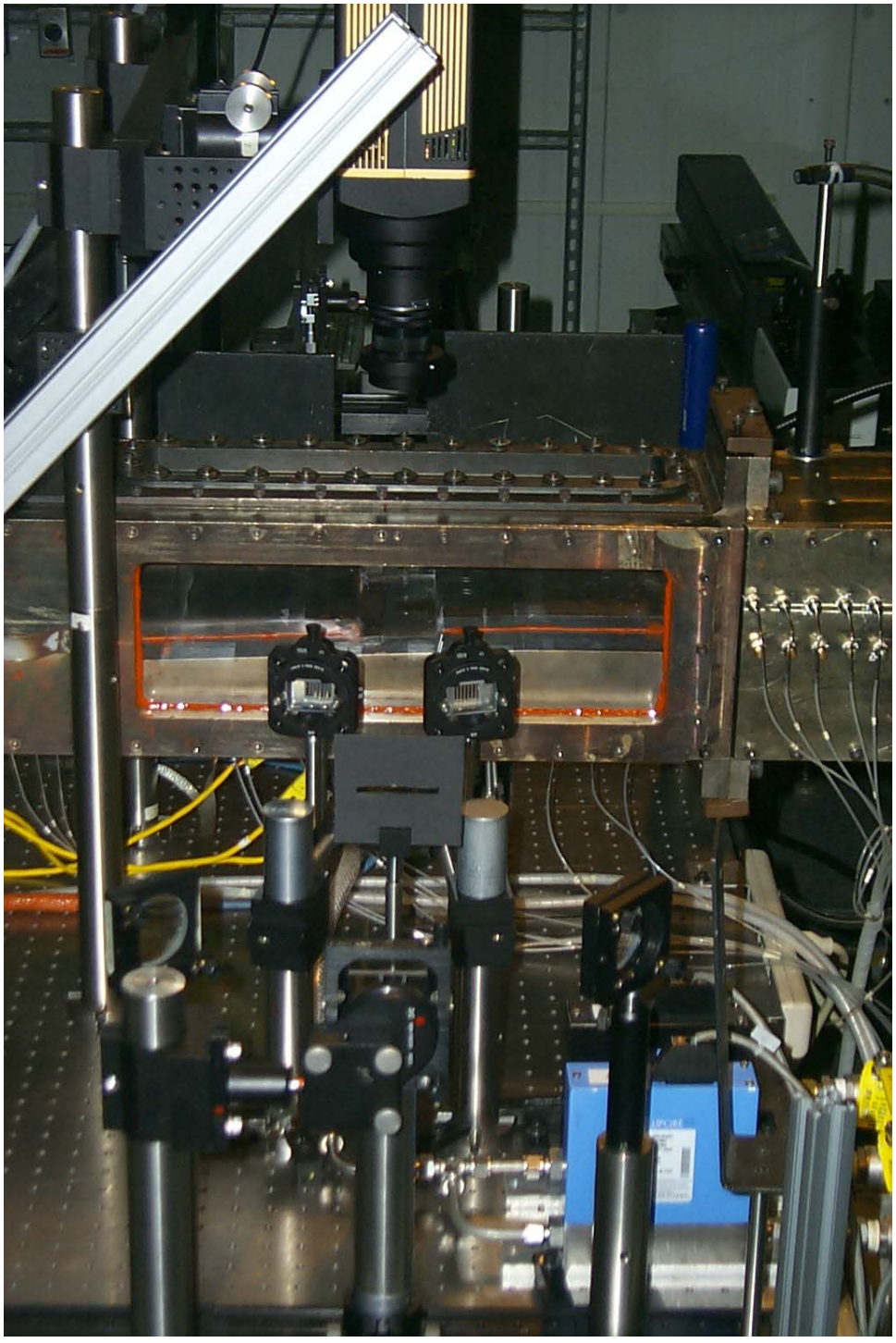

Fig. 4-6. Optical setup at the window to the cavity (flow is right to left).

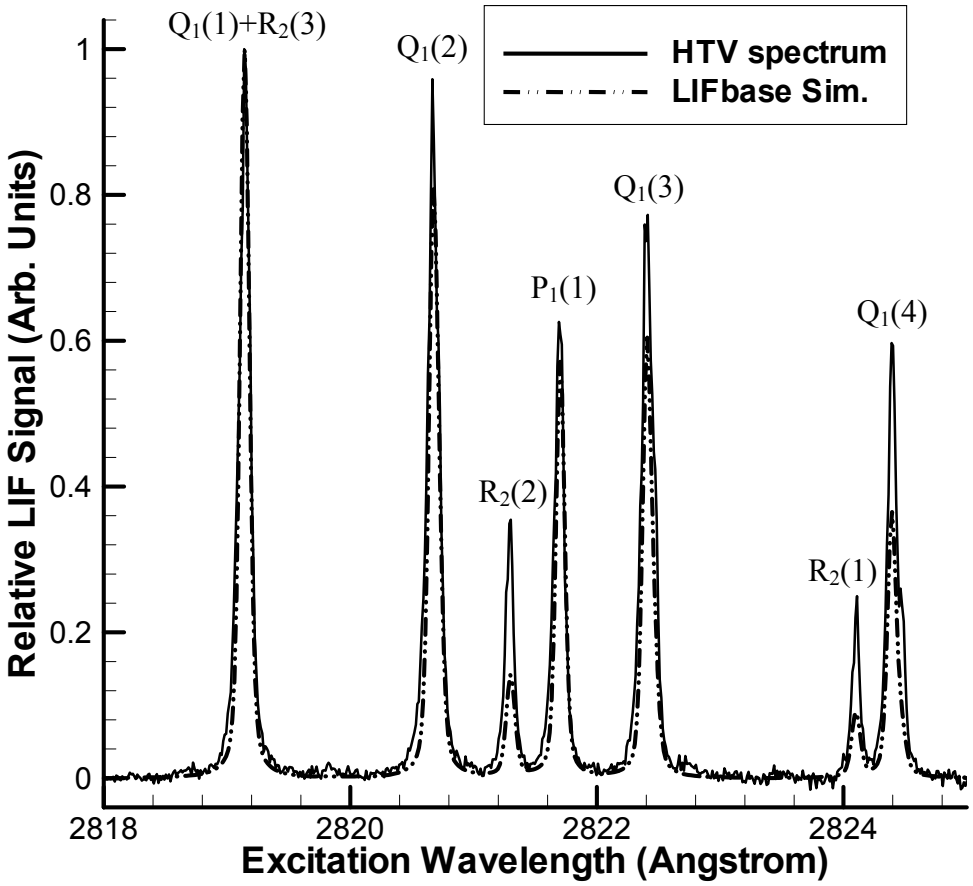

Fig. 4-7. Experimental and simulated excitation scans (relative to the $Q_1(1)$ signal) across OH A-X(1,0) transitions. Broadening of the simulated spectrum (T=295 K, LIFbase v. 2) was adjusted to match approximately the experimental spectrum; peak heights of the experimental and simulated $Q_1(1)+R_2(3)$ line were also matched. The experimental spectrum was derived from a sequence of 600 images, each image being the sum of 5 exposures of the grid at ~295 K and 745 Torr.

4.3 Post-processing Technique

A direct spatial image correlation technique has been developed at Michigan State University for estimating the Lagrangian displacement vector from image pairs based on molecular tagging diagnostics. This technique can be applied to grid arrangements, such as those created with hydroxyl tagging velocimetry, as long as there are spatial gradients along two (preferably orthogonal) directions (Gendrich and Koochesfahani 1996).

In this molecular tagging velocimetry (MTV) code, a small region surrounding a grid intersection in the undelayed image, referred to as the source window, is spatially correlated with a larger roam window in the delayed image. A visual representation of this description is shown in Fig. 4-8. A region, or grid intersection, is initially flow tagged at a time t_1 by an intersection pair of laser beams. Due to the flow velocity, the tagged region is displaced (Δx, Δy) to a new location at a later time $t_2 = t_1 + \Delta t$. The source window is specified about the initial tagged region in the undelayed image, and it is spatially correlated with the larger roam window, which is specified in the second (delayed) image. The spatial correlation coefficient between the intensity field of the source window and that of the roam window can be calculated as a function of the pixel displacement between them. The location of the peak of the correlation coefficient is identified as the displacement vector, which after division by the time delay between two images provides the estimate of the spatial average of the velocity within the source window.

Subpixel accuracy is achieved by using a multidimensional polynomial fit to the region near the correlation peak. Determining the displacement vector with the highestpossible sub-pixel accuracy allows for shorter time delays to be used between

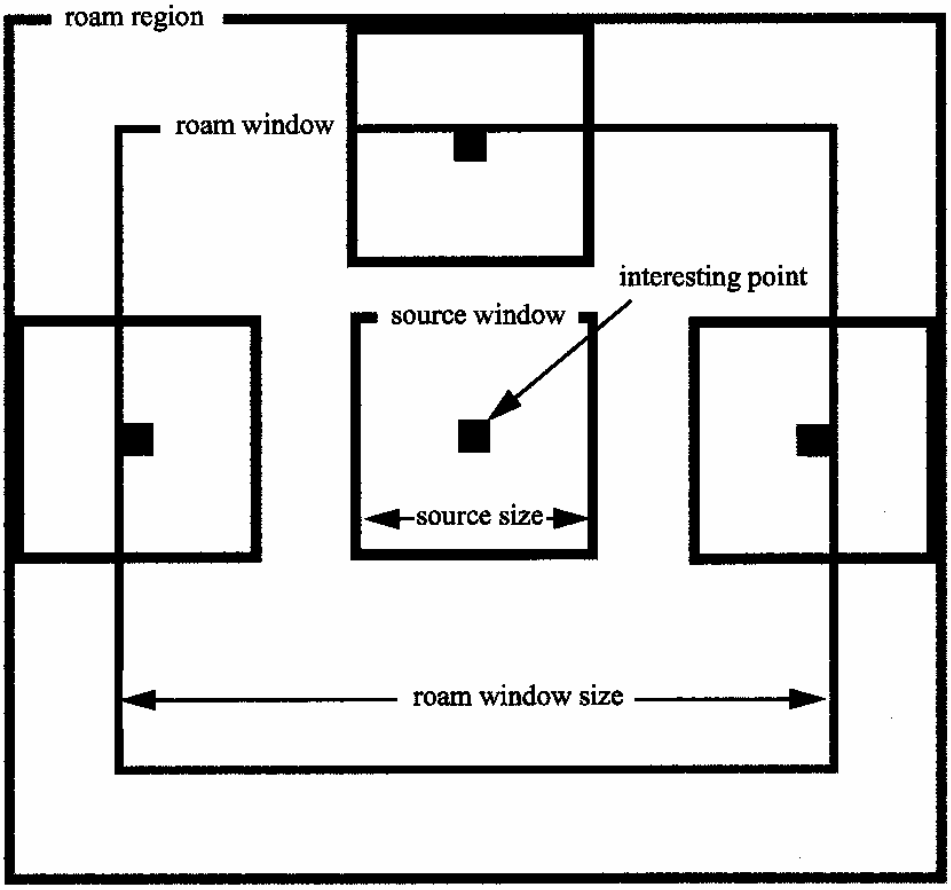

Fig. 4-8. Visual representation of the elements used in the molecular tagging velocimetry code (Gendrich and Koochesfahani 1996).

subsequent images there by increasing the dynamic range of the velocity measurements. This MTV code has many factors influencing its accuracy including: signal-to-noise ratio in the image pairs, image contrast, laser grid crossing angle, and the order of the polynomial fit for sub-pixel estimation of displacement.

Sub-pixel accuracy is the most important factor pertaining to the hydroxyl tagging velocimetry work at Wright-Patterson AFB. Gendrich and Koochesfahani (1996) ran simulations in which the signal-to-noise ratio is varied from 1 to 255; the contrast of the second image before adding noise is 104 in all cases. Figure 4-9 illustrates the displacement uncertainty results from this simulation for different values of intersection angle and S/N. The signal-to-noise ratio for our experiments in 2004 at WPAFB is about 10 for the OH lines, while the intersection angle is around 150^{o}. Therefore, the sub-pixel accuracy for this method using the HTV grid intersections is approximately 0.1.

When using the molecular tagging velocimetry code from Michigan State University, the data is obtained originally on an irregularly spaced measurement grid. Velocity vectors are calculated at the intersection of these spaced laser lines. In general, these lines are not uniformly spaced. To take advantage of standard data display and processing techniques, the MTV data can be remapped onto a grid with uniform spacing. The remapping is done by using a local least-squares fit to a two-dimensional second-order polynomial. Various images from HTV data taken at Wright-Patterson AFB have been remapped onto a regular grid to better show a visual representation of the flow field.

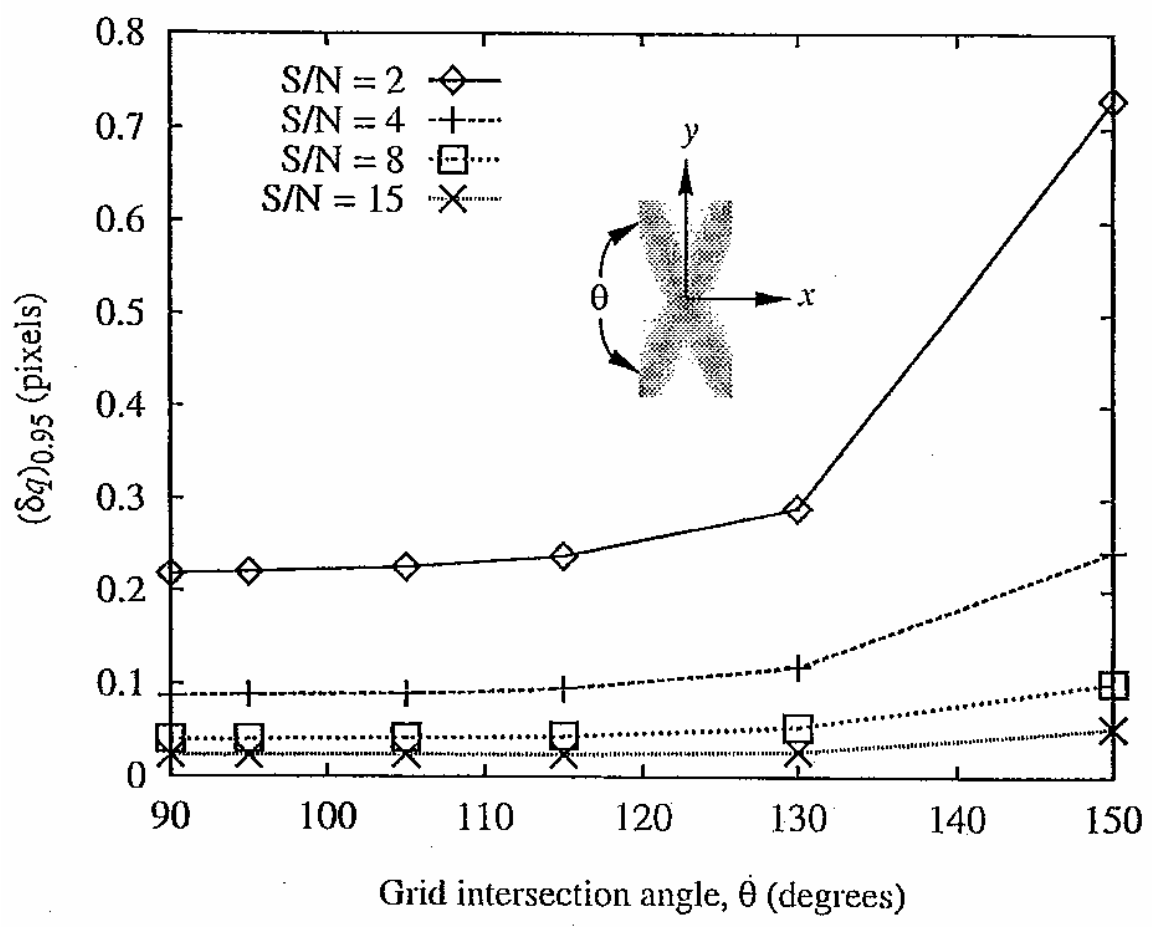

Fig. 4-9. Displacement sub-pixel accuracy versus grid intersection angle for different values of signal-to-noise ratio (Gendrich and Koochesfahani 1996).

4.4 Results

The hydroxyl tagging velocimetry measurements were made in the cavity flame holder in air with no fuel addition. Data was taken from the freestream (above the cavity) into the recirculation zone at the bottom of the flame holder. The conditions for the nonreacting flow are given in Table 4-1. Test A is the "low backpressure" condition in which the backpressure valve downstream of the test section is fully open. Test B is the "high backpressure" condition in which the backpressure valve is 64% closed. The "high backpressure" condition simulates the pressure rise from main-duct combustion. Under "low backpressure" conditions the tunnel flow above the cavity is largely free of shock waves. A shadowgraph single-shot image (200 μs exposure) of the Mach 2, non-reacting flow under low backpressure conditions is shown in Fig. 4-10 (Rasmussen et al. (2005). There is an obvious complex wave pattern above the cavity, and the curvature of the shock apparent at the leading edge displays its unsteady nature. There are also a number of other, weaker waves visible. These waves are inherent to the fact that there are pressure oscillations that occur with a wall cavity flameholder. Under "high backpressure" conditions, strong shocks appear above the cavity in the form of a shock train causing the shear layer to be deflected upwards (Gruber et al. 2004).

Since the tunnel air was dried, water was sprayed into the stagnation chamber to provide moist air and adequate OH planar laser-induced fluorescence signal levels for the hydroxyl flow tagging. Sufficient water was added to increase the relative humidity at Mach 2 isentropic conditions to about 32% (P = 22 kPa, T = 290 K). HTV measurements were made in the spanwise direction in the tunnel. The position of the measured OH grids

Table 4-1. Mach 2 flow with a wall cavity (2004).

Test	Mach No.	Stagnation Conditions		Isentropic Conditions Mach = 2		Air Mass Flowrate	Water Mass Flowrate	Back Pressure Valve	Cavity Bottom Wall Pressure
		P_o (kPa)	T_o (K)	P (kPa)	T (K)	(kg/sec)	(g/sec)	(%)	(kPa)
A	2	170	520	22	290	1.4	25	0	35
B	2	170	520	22	290	1.4	25	64	70

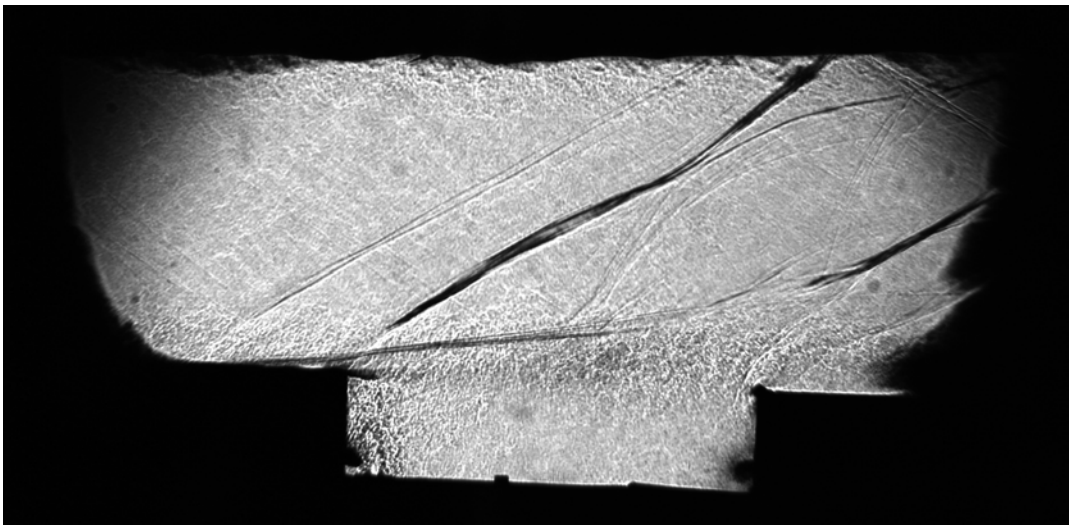

Fig. 4-10. Shadowgraph single-shot image over a rectangular cavity in a Mach 2 non-reacting cavity flow at low backpressure conditions.

in regards to the cavity walls is shown in Fig. 4-11. Examples of two-dimensional instantaneous velocity images from the HTV method are shown in Figs. 4-12, 4-13, 4-14, 4-15, and 4-16. Fig. 4-12 is an example of an un-delayed averaged HTV image used as the reference for the displaced grid patterns. The velocity vectors in Figs. 4-13, 4-14, 4-15, and 4-16 are shown on top of the displaced HTV grid pattern. In this work, the time delay is either 2 or 3 μs. For the low backpressure condition a delay of 2 μs was used for y = 15.65 mm to y = 0.41 mm, while a 3 μs delay was used for y = -2.13 mm to y = -12.3 mm. For the high backpressure condition a delay of 2 μs was used for y = 15.65 mm to y = -2.13 mm, and a delay of 3 μs was used for y = -4.67 mm to y = -12.3 mm. The irregular grid and regular grid spacing applied to the HTV measurements are shown in Figs. 4-13 and 4-14. The irregular grid pattern, or original grid pattern, shown on the left is fit with this procedure onto the regular grid shown on the right. The details of the procedure and its performance characteristics are given by Cohn and Koochesfahani (2000).

In the freestream above the cavity shown in Fig. 4-13, the velocity pattern is very uniform with a value of about 680 m/s (note reference vector of 700 m/s). The higher velocity (than expected for the Mach 2 nozzle) arises from the divergence of the bottom wall. In the cavity, the flow reverses, and the velocity pattern is much more variable as seen in Fig. 4-14. The velocities in the cavity are reversed with a negative velocity of up to about 200 m/s (note reference vector of 200 m/s).

The average signal-to-noise ratio of the single-shot images is about 7-13. As mentioned before, with a crossing angle of about 150 degrees, the center of the line crossings can be determined within 0.1 pixels or a displacement uncertainty of ± 16 μm

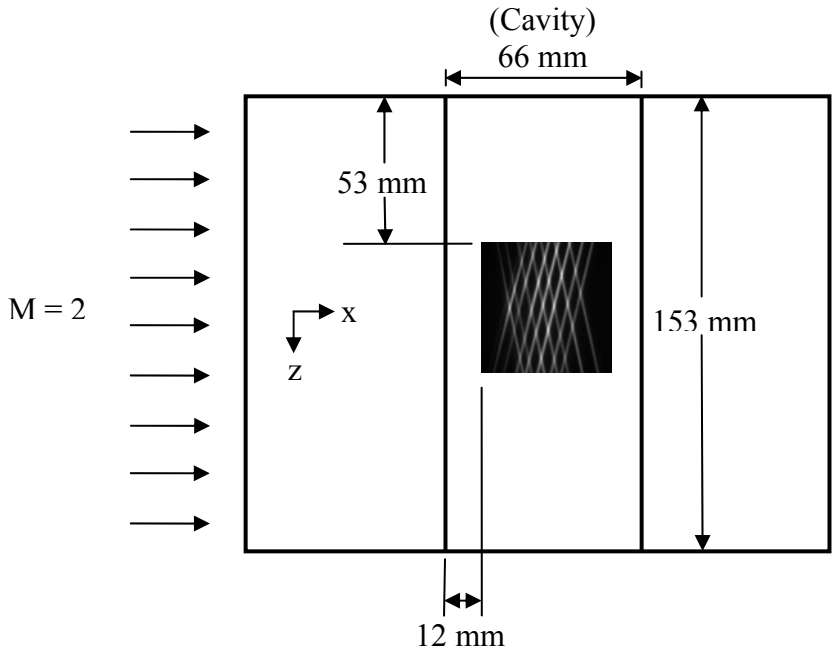

Fig. 4-11. Overhead schematic of the cavity, showing the position of the HTV images in regards to the cavity steps and test section walls.

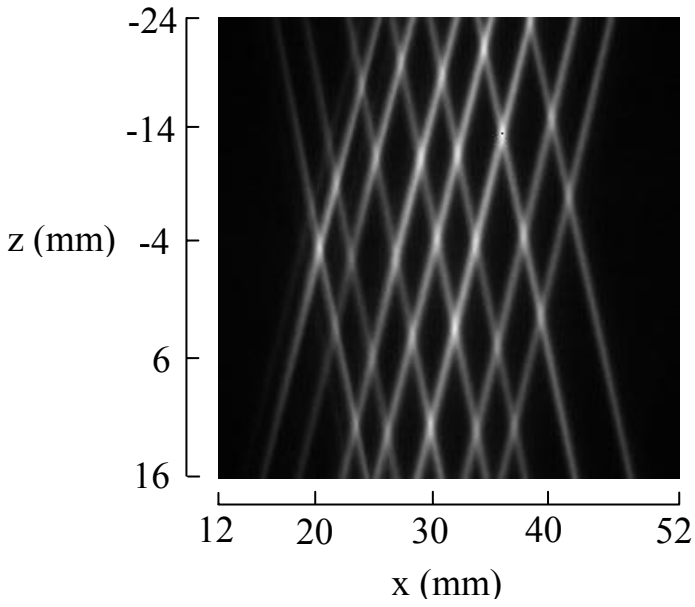

Fig. 4-12. Averaged un-delayed HTV image (at y = 15.65 mm, where z=0 is the centerline of the cavity and x=0 is at the front face of the cavity).

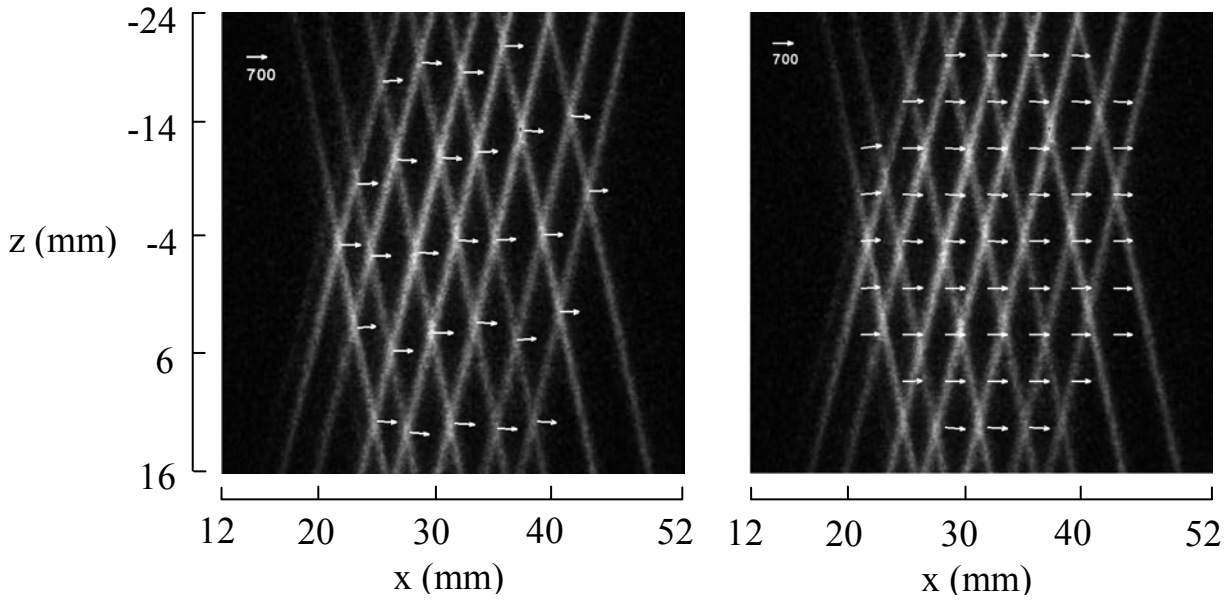

Fig. 4-13. Single-shot HTV images giving velocity fields with an irregular (left) and regular grid (right) in a Mach 2 non-reacting scramjet cavity flow at low backpressure conditions (at y = 15.65 mm, where z=0 is the centerline of the cavity and x=0 is at the front face of the cavity).

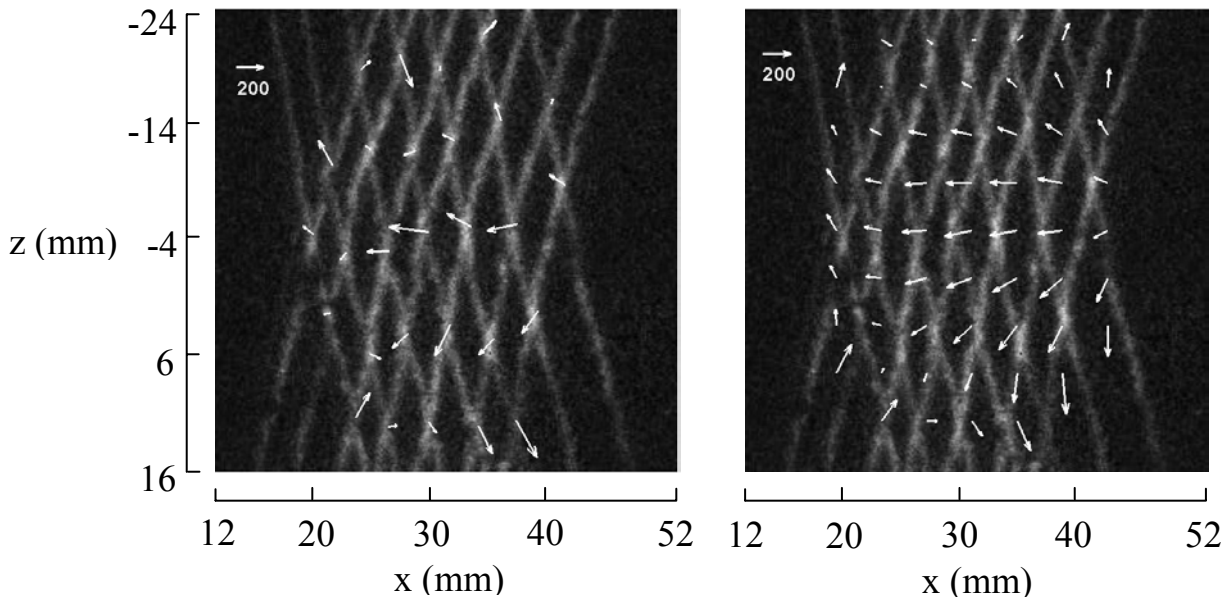

Fig. 4-14. Single-shot HTV images giving velocity fields with an irregular (left) and regular (right) grid in a Mach 2 non-reacting scramjet cavity flow at low backpressure conditions (at y = -4.67 mm, where z=0 is the centerline of the cavity and x=0 is at the front face of the cavity).

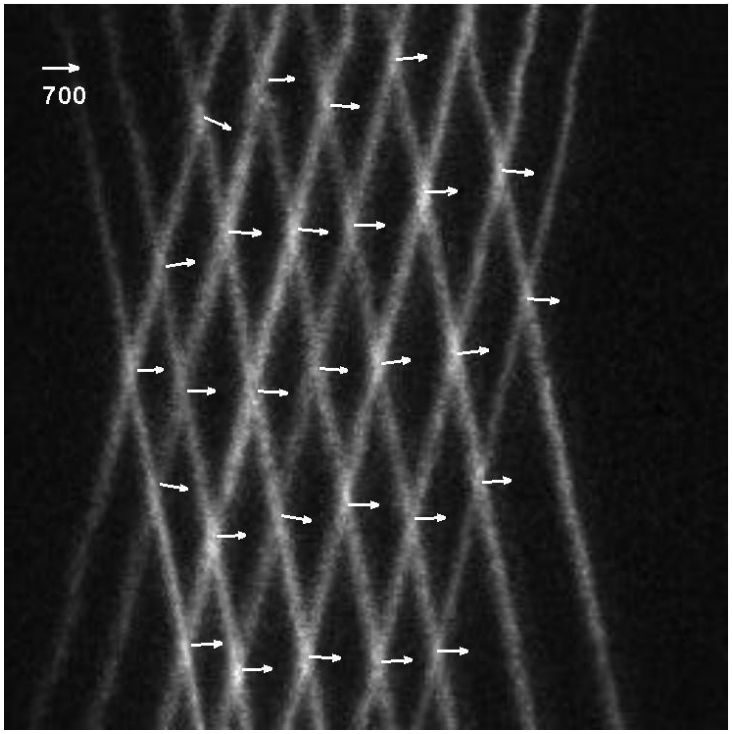

Fig. 4-15. Single-shot HTV image giving velocity field in a Mach 2 non-reacting scramjet cavity flow at high backpressure conditions (at y = 15.65 mm, where z=0 is the centerline of the cavity and x=0 is at the front face of the cavity).

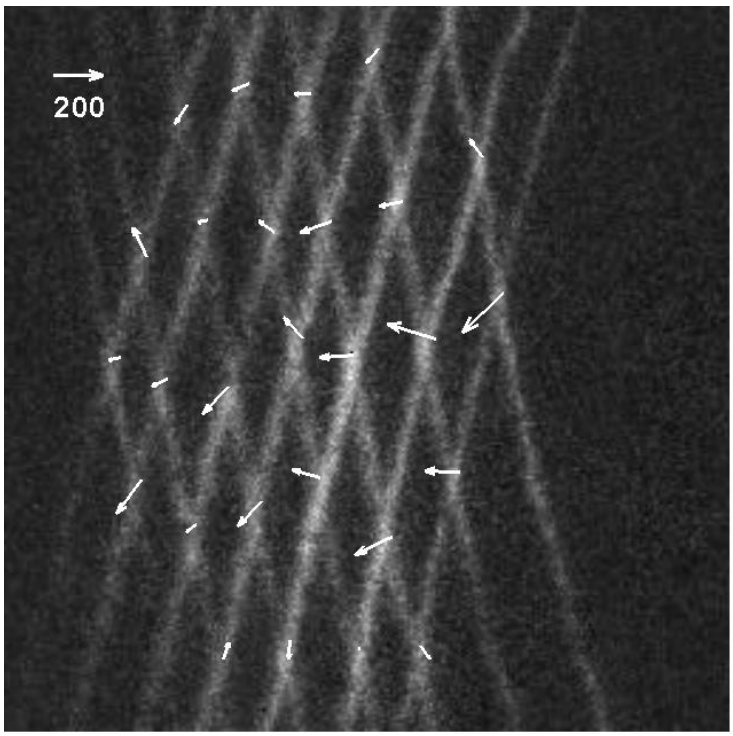

Fig. 4-15. Single-shot HTV image giving velocity field in a Mach 2 non-reacting scramjet cavity flow at high backpressure conditions (at y = -4.67 mm, where z=0 is the centerline of the cavity and x=0 is at the front face of the cavity).

according to previous calculations (Gendrich and Koochesfahani 1996). Thus the uncertainty of the velocity measurement due to the crossing-point determination is about 8 m/s for a 2 μs delay or 5 m/s for a 3 μs delay. The spatial resolution corresponding to the HTV velocity data ranges from approximately 2 pixels (.3 mm displacement) in the bottom of the cavity to approximately 9 pixels (1.4 mm displacement) in the freestream. It can be seen that longer delay times at a given position, and hence larger displacements, can provide better velocity data accuracy. The method is also limited by the timing accuracy which is about 20 ns for the 2 μs and 3 μs delays. Thus, with this technique one can achieve comparable relative uncertainty—about ± 1% for the full-scale displacement—to that with the PIV technique (which is limited in a similar fashion by correlation peak finding uncertainty).

The instantaneous HTV velocity images were analyzed to obtain mean and rms velocity profiles at the locations shown in Fig. 4-17. The mean velocity profiles at various streamwise (x axis) locations for the low backpressure case are shown in Fig. 4-18. Each data point is an average of 100 instantaneous values obtained from the images. Streamwise profiles are shown near the centerline of the tunnel from the freestream to down in the cavity. The velocities above the cavity are about 680 m/s and decrease in the shear layer and become negative (about -60 m/s) in the cavity. The shear layer profile appears typical of flows formed behind a rearward facing step (Pitz and Daily 1983). The shear layer width grows with downstream distance, as expected.

The rms velocities for the low backpressure case are shown in Fig. 4-19. The rms values in the freestream are as low as 15 m/s or about 2.2%. This rms value is due to a combination of freestream turbulence and measurement precision. Recall that the timing

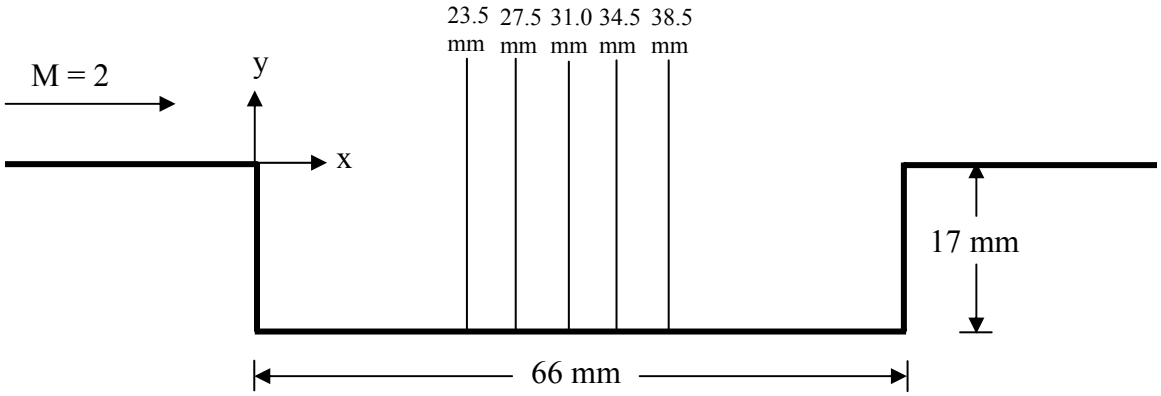

Fig. 4-17. Side-view schematic of the cavity, showing the profile locations along the x-axis.

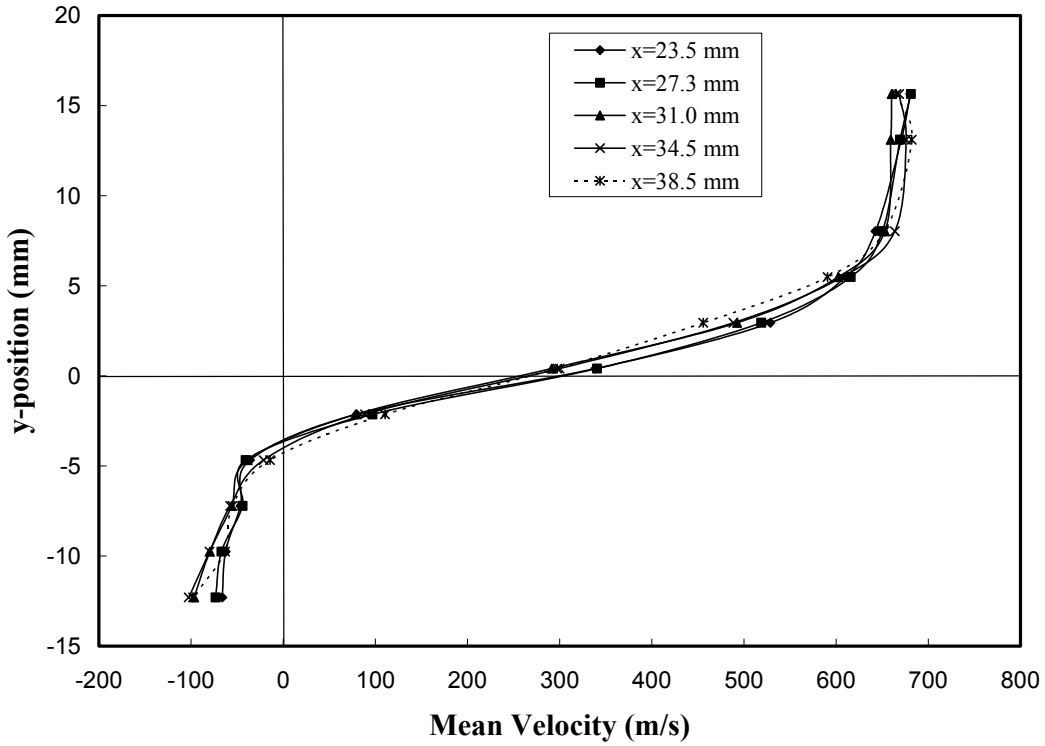

Fig. 4-18. Mean velocity profiles at different streamwise (x) locations showing the shear layer between the freestream and the cavity at low backpressure conditions (near centerline, z = -3.5 mm where z=0 is the centerline of the cavity and x=0 is at the front face of the cavity).

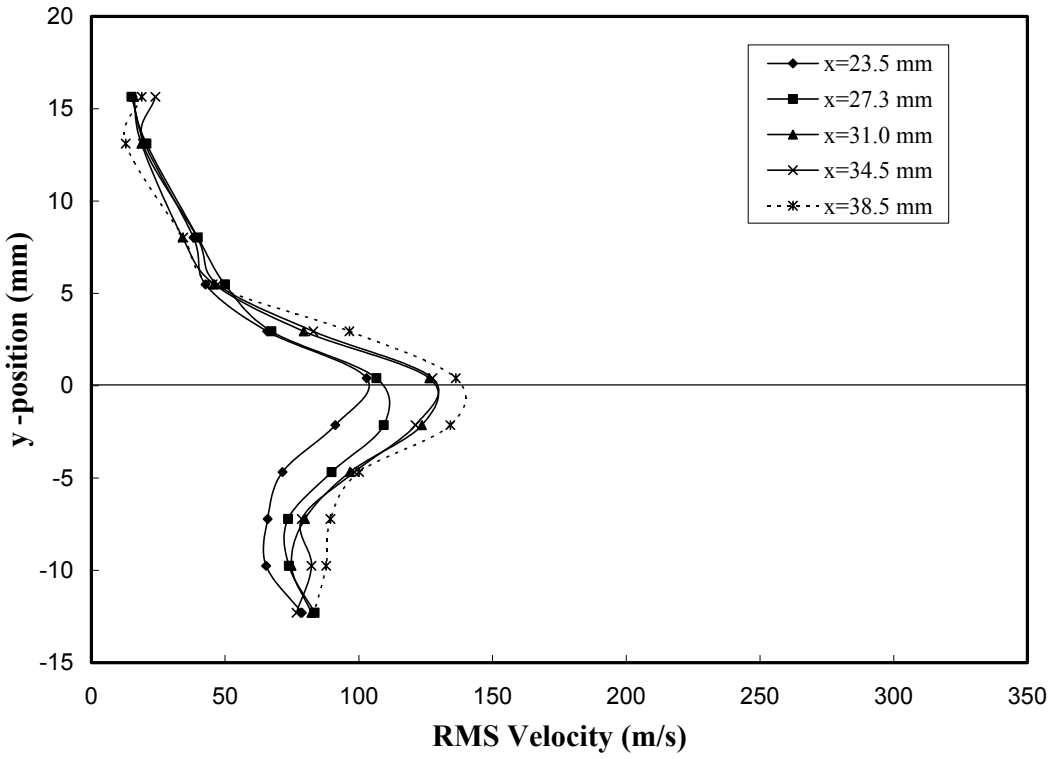

Fig. 4-19. Rms velocity profiles at different streamwise (x) locations showing the shear layer between the freestream and the cavity at low backpressure conditions (near centerline, z = -3.5 mm where z=0 is the centerline of the cavity and x=0 is at the front face of the cavity).

error is about ±1% of the typical 2 μs delay and the distance error is about 16 μm, equaling 8 m/s or about 1.2%; of course, the timing error could largely be eliminated byrecording with a photodiode the timing for each image. The rms values increase in the shear layer and decrease slightly in the cavity similar to what is observed in the flow behind a rearward facing step (Pitz and Daily 1983).

The mean and rms values for the high backpressure case are shown in Figs. 4-20 and 4-21. The profiles are drastically changed from the low backpressure case. Shock waves observed previously (Gruber et al. 2004) greatly modify the mean and rms values of the velocity. These profiles do not correspond to those seen in subsonic flows behind a rearward facing step (Pitz and Daily 1983). In this unsteady compressible flow with shocks, the shear layer is deflected upwards (Gruber et al. 2004). This results in a mean velocity profile that appears almost linear above the cavity. The rms values are highest above the cavity where shocks have been previously observed by Gruber et al. (2004).

Mean and rms velocity profiles at various spanwise (z axis) locations denoted in Fig. 4-22 for the low backpressure case are shown in Figs. 4-23 and 4-24. The x-component (streamwise) of velocity is uniform in the spanwise direction with vertical location from the freestream to the shear layer as seen in Fig. 4-23. However, at about y = -5 mm, the velocity field becomes less uniform in the spanwise direction with the rms velocity rising up to almost 200 m/s before the flow regains spanwise uniformity at the bottom of the cavity (y = -13 mm). As shown in Figs. 4-14 and 4-23, the greatest recirculation occurs around the center of the grid (z = -4.1 mm) and decreases away from the centerline.

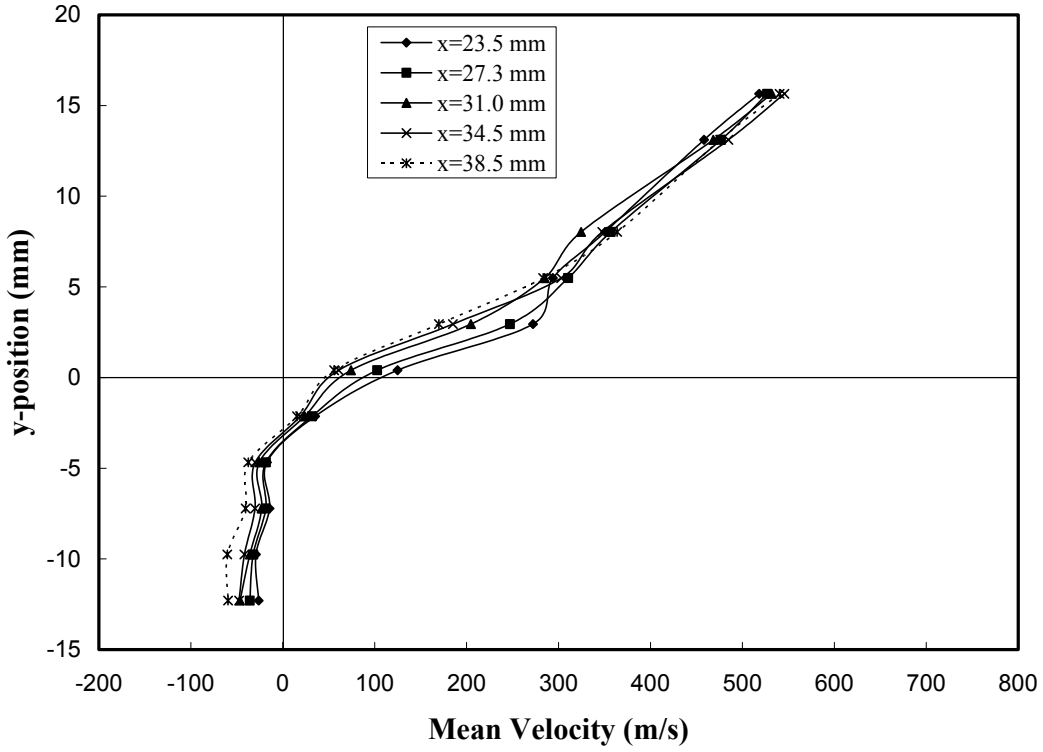

Fig. 4-20. Mean velocity profiles at different streamwise (x) locations showing the shear layer between the freestream and the cavity at high backpressure conditions. (Near centerline, z = -3.5 mm where z=0 is the centerline of the cavity and x=0 is at the front face of the cavity).

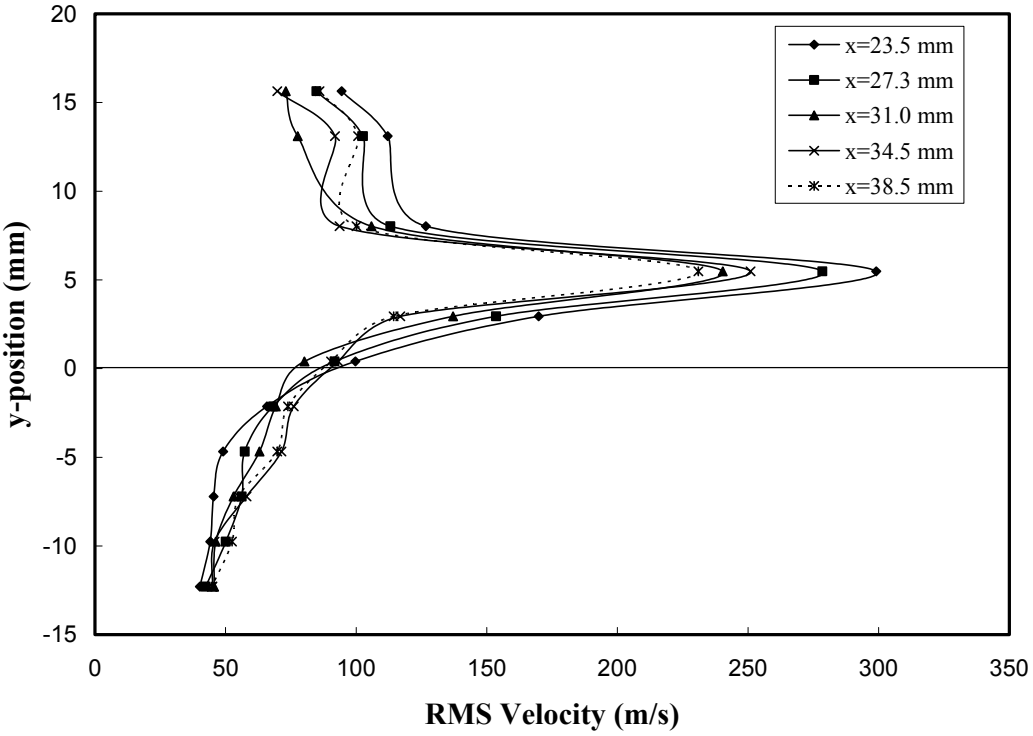

Fig. 4-21. Rms velocity profiles at different streamwise (x) locations showing the shear layer between the freestream and the cavity under high backpressure conditions. (Near centerline, z = -3.5 mm where z=0 is the centerline of the cavity and x=0 is at the front face of the cavity).

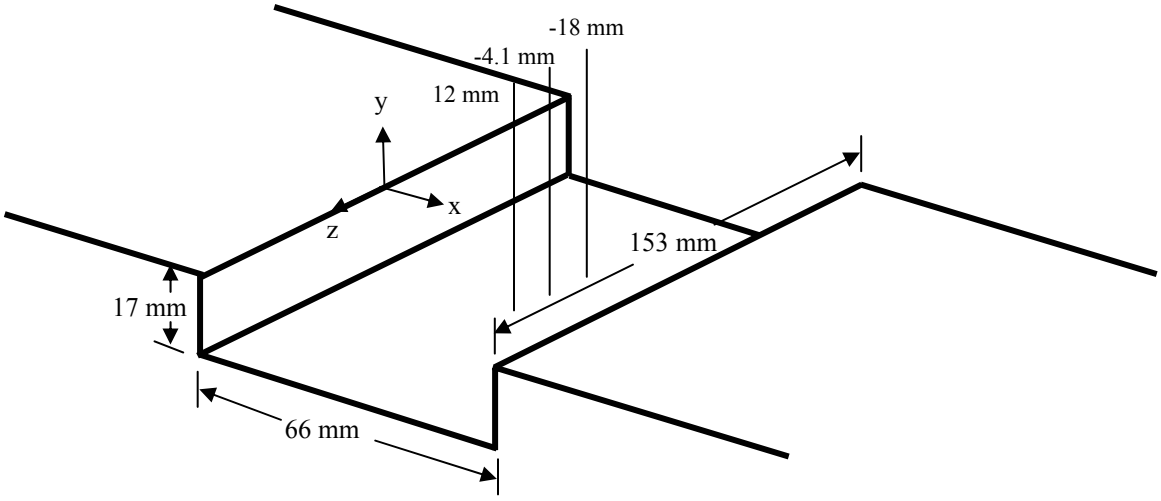

Fig. 4-22. Schematic of the cavity, showing the profile locations along the z-axis.

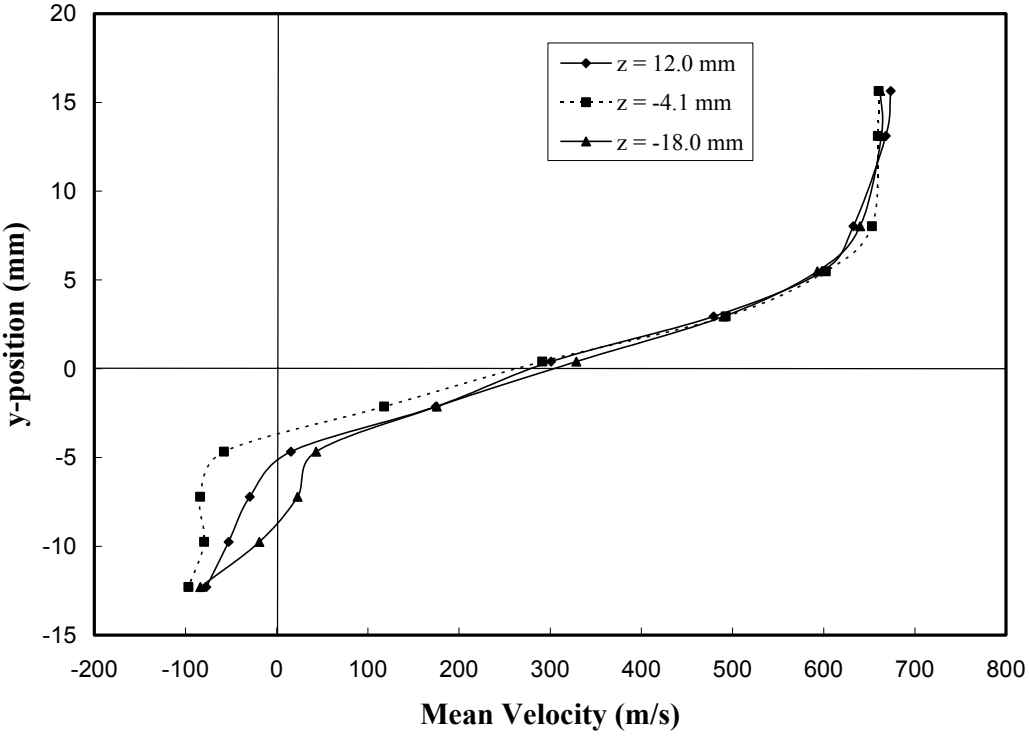

Fig. 4-23. Mean velocity profiles at three spanwise (z) locations showing the flow uniformity between the freestream and the cavity under low backpressure conditions (approximately x = 31 mm; x=0 is the front face of the cavity and z=0 is the centerline of the cavity).

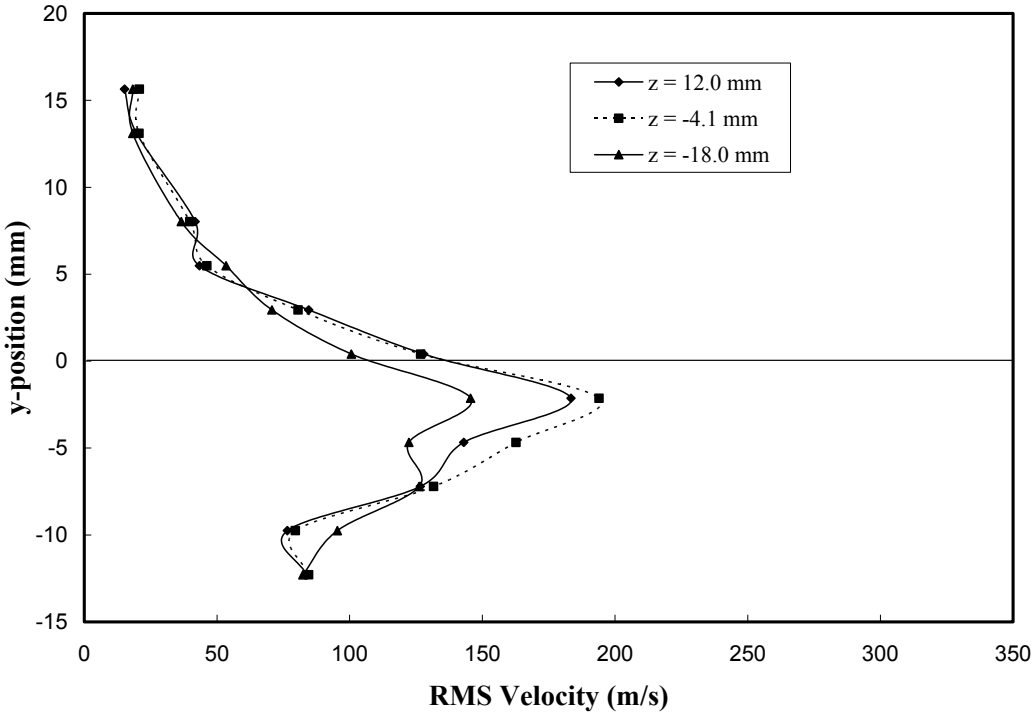

Fig. 4-24. Rms velocity profiles at three spanwise (z) locations showing the flow uniformity between the freestream and the cavity under low backpressure conditions (approximately x = 31 mm where x=0 is the front face of the cavity and z=0 is the centerline of the cavity).

CHAPTER V

HYDROXYL TAGGING VELOCIMETRY AT WRIGHT-PATTERSON AIR FORCE BASE (2005)

5.1 Objectives

Following up on the hydroxyl tagging velocimetry experiments conducted in 2004, there were certain aspirations and additions to the work that needed to be addressed in 2005. Once again, HTV experiments were conducted at the supersonic flow facility in Research Cell 19 at the Air Force Research Laboratory in the Propulsion Directorate at Wright-Patterson Air Force Base. There were three main objectives for the experiments conducted in 2005: 1) improve the grid optics used in the test by purchasing different sized cylindrical lenses to create a larger number of hydroxyl lines in the flow; 2) collect velocity data spanning the entire cavity flameholder from the front step to the rear step; and 3) demonstrate hydroxyl tagging velocimetry in reacting supersonic flow.

Prior to the tests at Wright-Patterson, new cylindrical lenses were purchased as a means to increase the crossing points and subsequent vector flow representation. The original grid optics consisted of 7 fused silica cylindrical lenses (3 mm thick with a 300mm f.l.) in each optic to produce a 7x7 grid pattern. New cylindrical lenses were purchased to increase the number of grid lines in the flow. The new grid optics consist of 11 fused silica cylindrical lenses (2 mm thick with a 300 mm f.l.) in each optic to produce an 11x11 grid pattern with ~ 120 crossing points as shown in Fig. 5-1. The grid optics were used at WPAFB in Research Cell 19 to attempt accomplishment of the remaining two objectives.

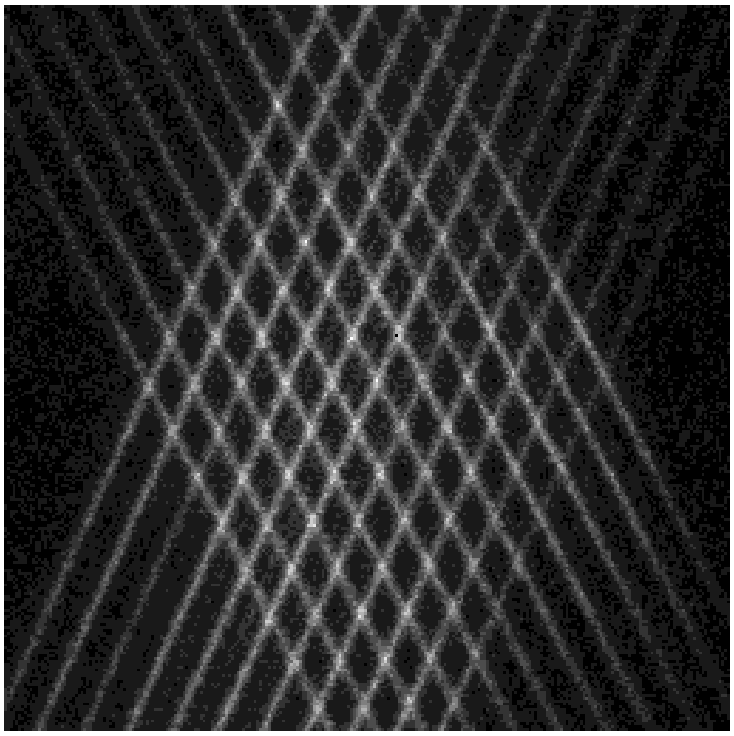

Figure 5-1. Example of single-shot HTV image in Mach 2 non-reacting scramjet cavity flow using the new grid optics (11 cylindrical lenses in each optic).

5.2 Experimental System

The experimental system did change slightly from that of 2004 with the need to collect data from step to step. The air flow rate was once again 1.4 kg/s. In addition, the test section, dye laser setup and specifications, and camera specifications remained the same, with the cavity test configuration also being identical to that used in 2004. However, the ArF excimer laser setup had to be altered to be able to achieve accessible angles through the windows to induce fluorescence with the greatest amount of crossing points and least amount of laser scattering. A schematic of the HTV system is shown in Fig. 5-2. Three different configurations were used to proceed downstream of the leading edge of the cavity, but this only consisted of changing the angles of the grid optics to allow for accessible measurements. The basis for the new setup resides in the ArF excimer laser beam (20 mm high by 10 mm wide, 150 mJ/pulse, broadband, 1 nm bandwidth) being split into two beams, one traveling under the test section to the other side, and the other traveling up and staying on the same side of the configuration. This provides adequate crossing angles for the written lines in the flow regime across the cavity. A side view of one of the setups is shown in Fig. 5-3. The laser grids come in from both sides of the test section with the camera mounted above the tunnel. Each of the laser beams was sent through the new grid-forming optics to produce two sets of eleven beams each. The grid optics again consist of two major components placed very close together: a 300 mm focal length cylindrical lens (25 mm x 40 mm) and this time a stack of cylindrical lenses (20 mm wide by 2 mm high). The beam diameter was about 0.3 mm in the measurement zone. With the ArF excimer laser still operating broadband instead of narrowband, much of the beam was still absorbed by O_2.

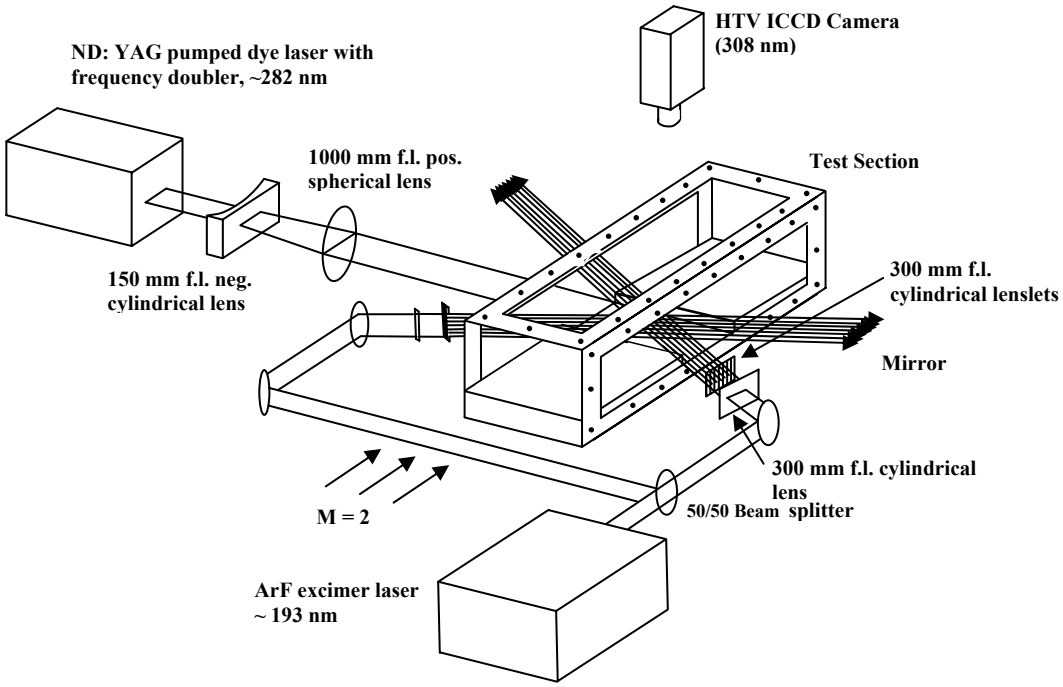

Fig. 5-2. Schematic of the HTV experimental system (2005).

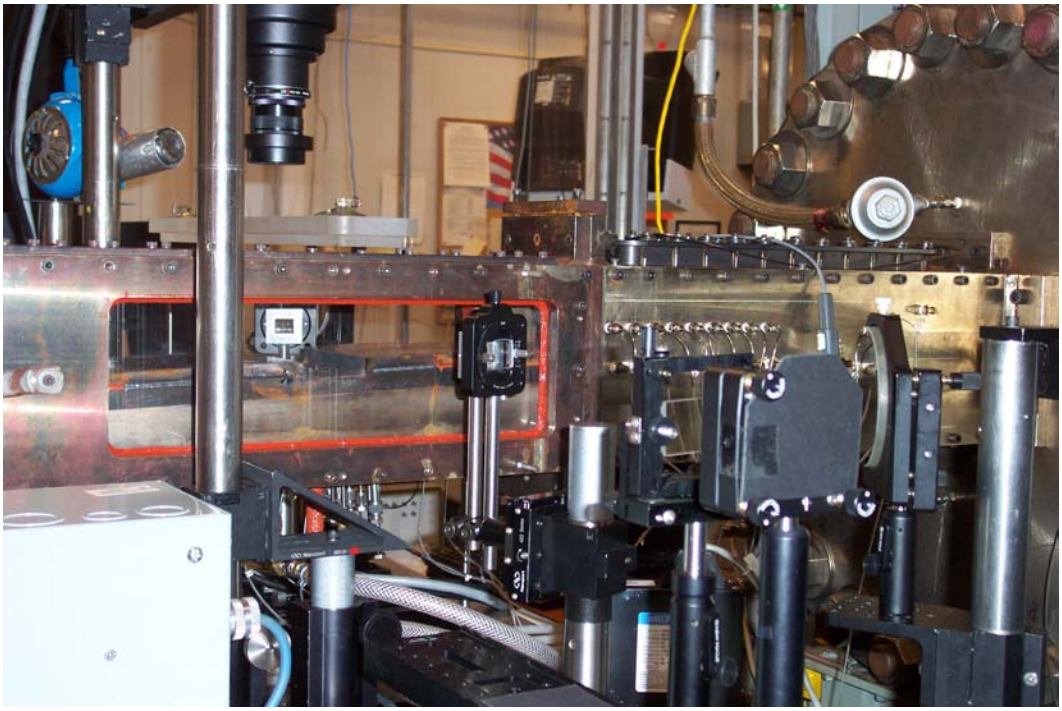

Fig. 5-3. Grid optics setup (300 mm focal length cylindrical lens in front of a stack of eleven 300 mm cyldindrical lenses).

5.3 Results – Nonreacting Flow

HTV measurements were again made in air with no fuel addition to provide velocity data across the whole length of the cavity. The three different non-reacting flow conditions used while testing are given in Table 5-2. Tests A and B are the low-backpressure cases, where the backpressure valve downstream of the test section is fully open. Test A used a tunnel stagnation pressure of 170 kPa, while Test B used a tunnel stagnation pressure of 345 kPa. Test C is the high-backpressure condition, where the backpressure valve is approximately 60 % closed. Again, the high-backpressure condition simulates the pressure rise from main-duct combustion. Strong shocks appear in the cavity under high-backpressure, while under low-backpressure conditions the tunnel is basically free of any shocks.

Dry air from the compressors used to run the wind tunnel did not contain adequate H_2O to achieve strong OH signals for hydroxyl tagging velocimetry. So, water had to be sprayed into the stagnation chamber to provide moist air. Water flowrates varied from 17 g/s to 25 g/s to improve the OH signal with no condensation or water droplets forming on the windows or in the flow. HTV measurements were made along the length of the cavity, while traveling vertically into the flameholder at each position.

The data from these tests is currently being analyzed using the spatial correlation technique developed by Gendrich and Koochesfahani (1996). Figs. 5-4, 5-5, and 5-6 are examples of two-dimensional instantaneous velocity images from the HTV method utilizing the new 11 x 11 grid pattern.

Table 5-1. Mach 2 flow with a wall cavity (2005).

Test	Stagnation Conditions		Isentropic Conditions Mach 2		Air Mass Flow Rate	Back Pressure Valve
	P_o	T_o	P	T		
	(kPa)	(K)	(kPa)	(K)	(kg/sec)	(%)
A	170	520	22	290	1.4	0
B	345	520	44	290	1.4	0
C	170	520	22	290	1.4	60

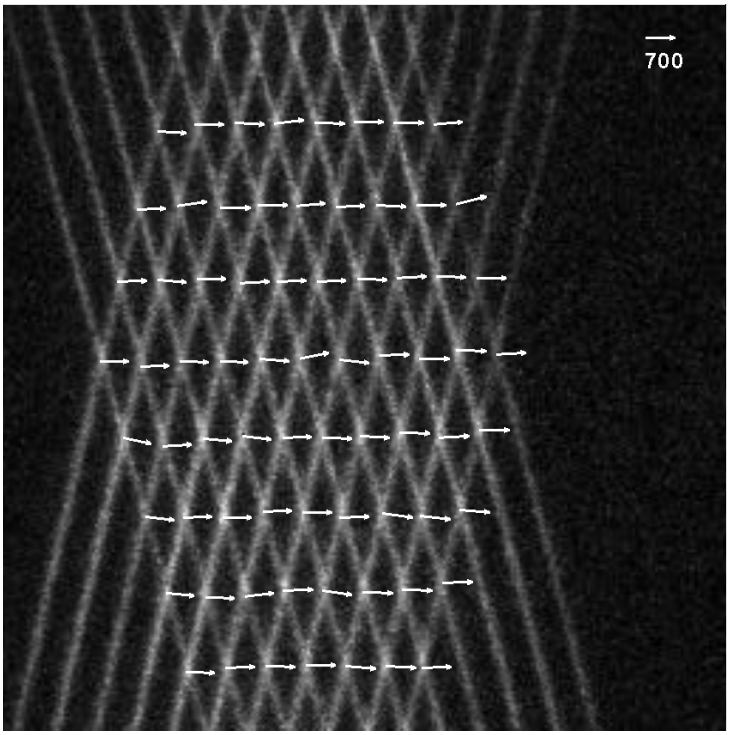

Fig. 5-4. Single-shot HTV image giving velocity field with an irregular grid in a Mach 2 non-reacting scramjet cavity flow for Test A at low stagnation pressure and low backpressure conditions at y = 15.65 mm (average velocity = 701 m/s).

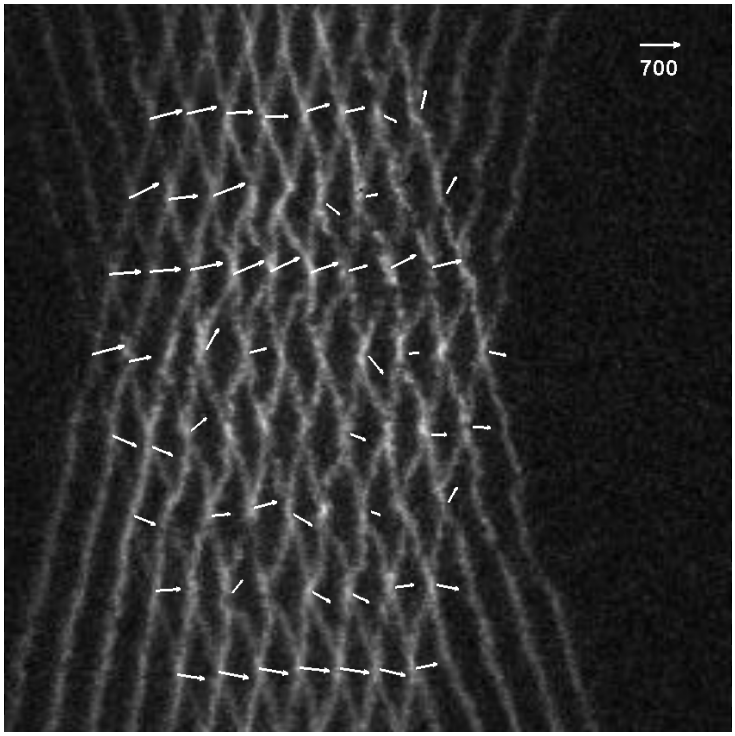

Fig. 5-5. Single-shot HTV image giving velocity field with an irregular grid in a Mach 2 non-reacting scramjet cavity flow for Test A at low stagnation pressure and low backpressure conditions at y = 2.95 mm (average velocity = 298 m/s).

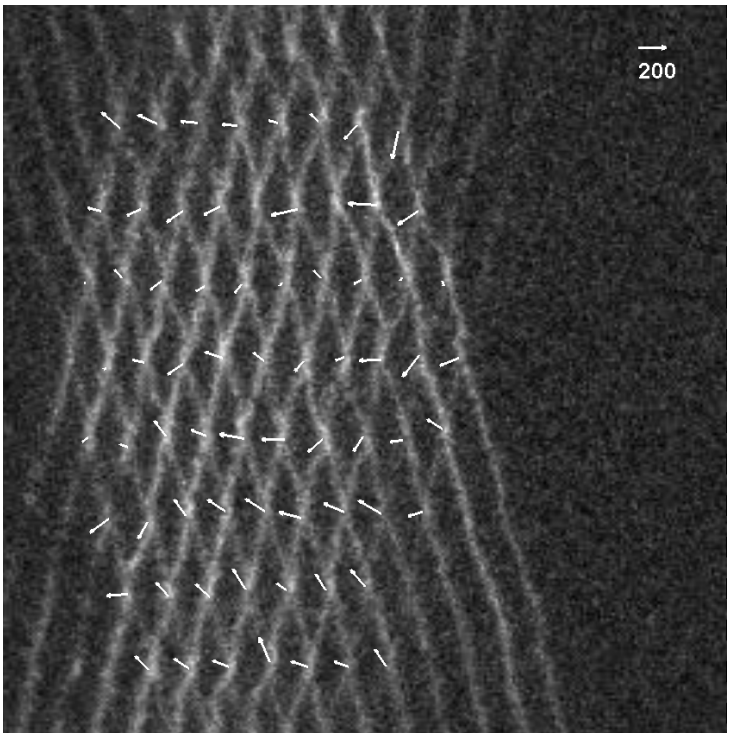

Fig. 5-6. Single-shot HTV image giving velocity fields with an irregular grid in a Mach 2 non-reacting scramjet cavity flow for Test A at low stagnation pressure and low backpressure conditions at y = -9.75 mm (average velocity = -90 m/s).

5.4 Results – Reacting Flow

HTV tests were conducted in reacting supersonic flow at Wright-Patterson Air Force Base in Research Cell 19. However, narrowband operation for the ArF excimer laser could not be achieved. Narrowband operation would have supplied a stronger OH signal, and allowed for the minimization of O_2 absorption through tuning of the narrow line output. Despite the laser only operating in broadband mode, reacting images were still obtained. Fig. 5-7 shows an averaged HTV image of 100 single-shots images in reacting ethylene Mach 2 flow. The HTV grid can be seen but the image is not distinct. HTV images were also recorded in a propane-air flame at ambient conditions with no flow to check the viability of reacting measurements. Fig. 5-8 is a single-shot HTV image of a propane flame in stagnant room air. The grid pattern is very discernable. Further tests in combustion will be undertaken at Vanderbilt. The ArF excimer laser is now in narrowband operation and measurements will be made in an ethylene-air flame to simulate the ethylene-fueled scramjet flow.

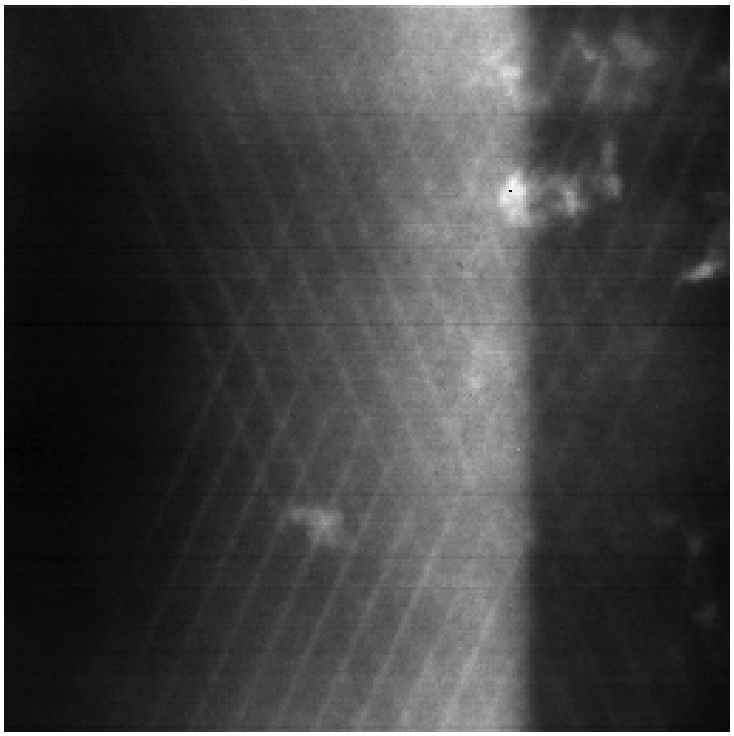

Fig. 5-7. Averaged HTV image in an ethylene flame at the aft step of the cavity.

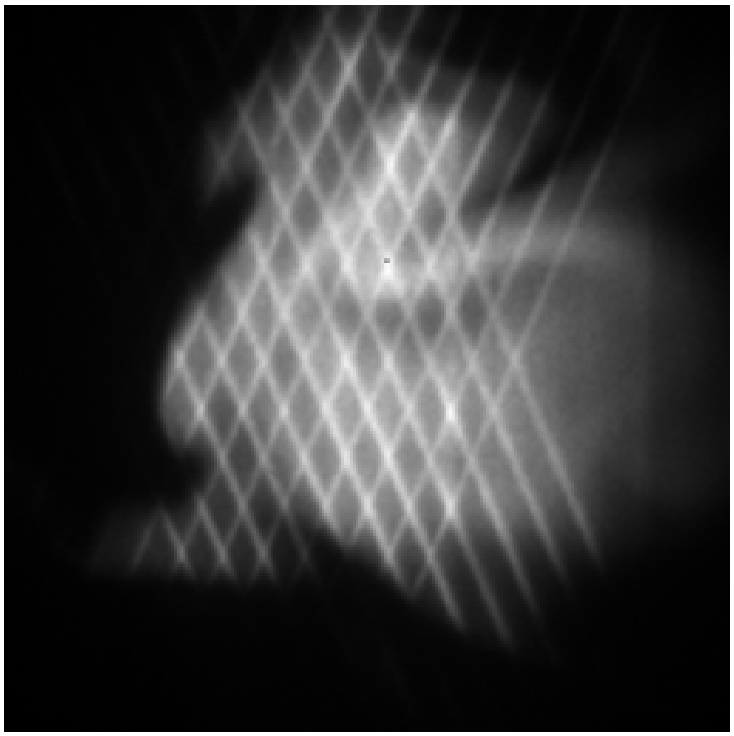

Fig. 5-8. Single-shot HTV image in a propane flame.

CHAPTER VI

FUTURE HYDROXYL TAGGING VELOCIMETRY WORK

6.1 Introduction

The ultimate scope of the HTV experiments conducted at Wright-Patterson Air Force Base was to demonstrate this technique in supersonic flow as a means of legitimizing the method for high temperature, high speed flow. The major goal in attempting to fully understand and explore a flow field is to apply our understanding and experience with hydroxyl tagging to the APTU facility at Arnold Engineering Development Center in Tullahoma, TN. Funding from AEDC has allowed for extensive testing and preparation in order to meet the needs of modelers and experimentalists in the hypersonic missile program at the Air Force base. Accurate velocity measurements in this Mach 8 wind tunnel could be a valuable resource in the continued desire to advance the hypersonics program in the United States. In addition to applying HTV to a real ramjet facility at WPAFB, additional tests and calculations have been run in anticipation for velocity testing at APTU. They include: 1) developing strategies and methods to reject particle and water vapor droplet scattering expected in the APTU facility; 2) developing strategies to make the HTV method vibration proof by obtaining both the HTV images in ~ 1 μs; 3) studying the lifetime of molecular tags (temperature, pressure, and molecular diffusion effects) in the APTU facility; and 4) analyzing the scaling issues associated with applying HTV to the APTU facility at AEDC.

6.2 Discussion

Light scattering from particles is a major concern in the hydroxyl tagging velocimetry method. When "tagging" (or exciting) the dissociated OH in the flow, laser light can scatter from particles and interfere with the image. The grid of ArF-generated "lines" of OH are imaged by laser-induced fluorescence of OH using a Nd:YAG pumped dye laser (frequency doubled) that produces either 282 nm or 308 nm laser radiation. When 308 nm laser light is used to excite the transition, the OH emission at 308 nm excited by the laser will overlap with light scattered from other erroneous particles in a test area. To avoid this problem, the OH can be excited by 282 nm laser light, another strong OH band, to ensure that the only fluorescence at 308 nm from the OH is recorded. This method was used successfully at Wright-Patterson AFB and can easily be implemented with the right filters at AEDC.

In typical hydroxyl tagging velocimetry, the time in between exposures allows for mechanical vibration in the setup to affect the displacement measurements. Double-pulse HTV is a method used to negate any interference or error that can occur between these exposures in a tagging experiment due to this mechanical vibration. With double-pulse HTV, the ICCD camera takes a double exposure in a time period (1-5 μs) that is much shorter than the characteristic mechanical vibrational time. An experiment to demonstrate this technique was conducted at Vanderbilt. The setup for this method is shown in Fig. 6-1. The air jet outlet is 1.8 mm in diameter. The upstream air pressure is 57 psig, and the air is emitted at room temperature. Quite different from typical HTV, the ArF excimer laser creates an un-delayed grid image through O_2 fluorescence, while the dye laser fluoresces the OH moving in the flow to expose a delayed grid image. O_2

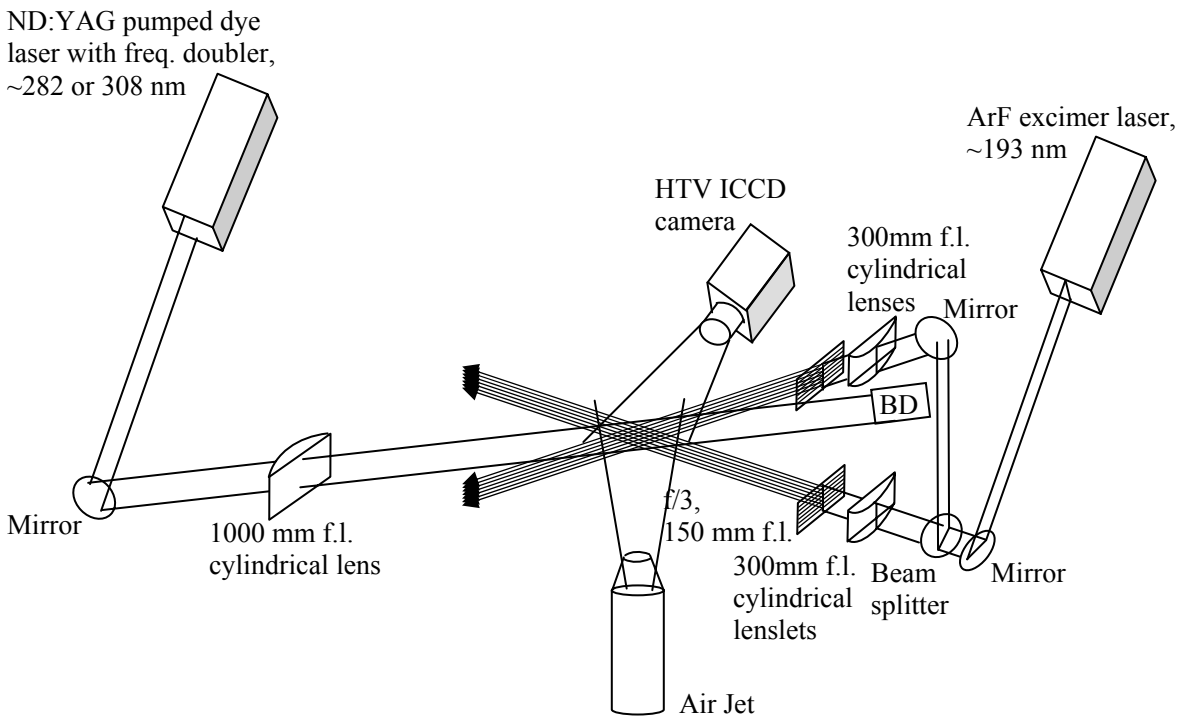

Fig. 6-1. Schematic of the double-pulse HTV experimental system.

and OH are fluoresced at slightly different wavelengths. Therefore, a good combination of filters on the camera lens must be obtained to fully capture both grids. In this case, both the UG-5 and WG-280 filters together were found to work best. The subsequent image, as shown in Fig. 6-2, contains both the original grid and the displaced grid for a short time delay of 5 μs. In faster flows, the delayed grid would be more distinguishable.

As mentioned earlier, one of the ultimate objectives of this work is HTV measurements in the APTU facility at AEDC where the scramjet prototypes will be tested. To obtain accurate velocity field measurements, the molecular tag of hydroxyl must have a lifetime long enough for there to be visible fluorescence over an adequate delay. The more discernable the images, the more accurate the post-processing is. Fig. 6-3 and 6-4 show OH lifetime measurements in the APTU nozzle at M = 5 computed with Chemkin software. The two cases (with no supplemental oxygen and with supplemental oxygen) are based on measurements in the APTU facility provided by Powell (1983). The flow conditions for each case are shown in Table 6-1, while the flow compositions are shown in Table 6-2. The four mechanisms noted on the plots in Figs. 6-4 and 6-5 (GRI-Mech 3.0 (Smith et al. 2005), San Diego (University of California San Diego 2003), nC_4H_{10} Mech (Marinov et al. 1998), iso-Octane Mech. (Curran et al. 2002)) provide slightly different product compositions. The HTV data under supersonic conditions are taken with a 2 μs or 3 μs delay. As can be seen from the figures, using any of the four mechanisms to model the combustion, over 50 % of the OH is still present at these delays. This provides more than adequate fluorescence for post-processing.

Finally, the magnitude and scale of the APTU facility poses a great challenge to using the HTV technique. With limited accessibility and space to set up the laser and

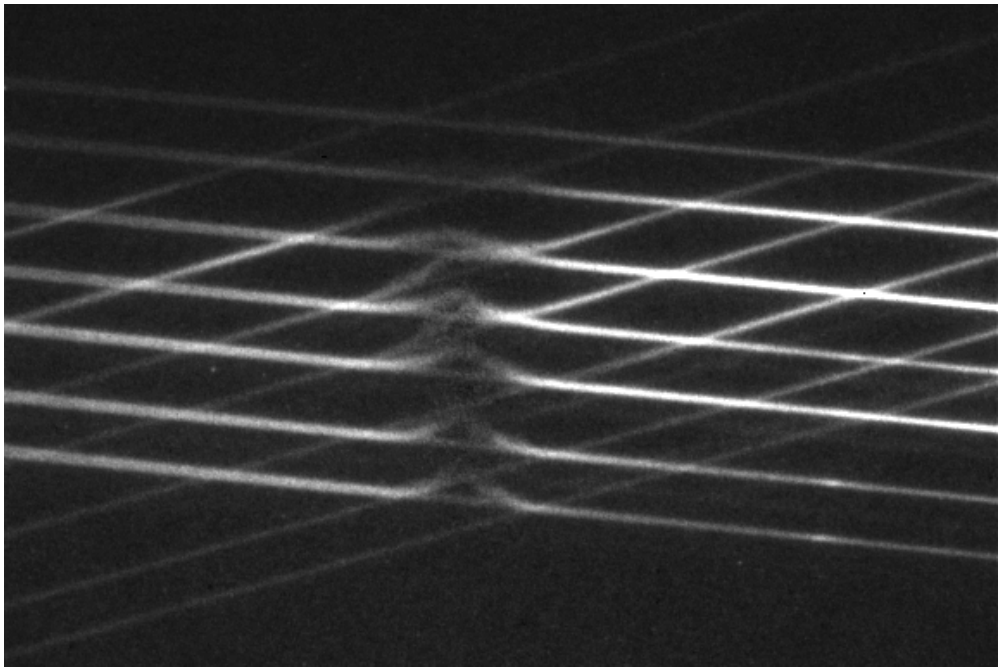

Fig. 6-2. Double-pulse HTV image (5 μs delay)

Table 6-1. APTU conditions

Case	Stagnation Conditions		Isentropic Conditions @ M=5	
	P_o (MPa)	T_o (K)	P (kPa)	T (K)
1 (no supplemental oxygen)	9.7	1778	18	314
2 (supplemental oxygen)	9.7	1778	18	314

Table 6-2. Composition of fuel/air mixture in APTU stagnation chamber (nominal conditions, P_o = 9.7 MPa, T_o = 1778 K)

	Case 1	Case 2
O_2	13.64%	20.45%
Ar	0.91%	0.88%
CO_2	3.77%	1.99%
H_2O	4.85%	2.45%
CO	0.11%	0.02%
NO	0.0016%	0.0061%
CH_3	0.00008%	0.00016%
CH_4	0.00064%	0.13%
C_2H_4	0.00039%	0.00079%
C_2H_6	0.00083%	0.0017%
C_3H_8	0.00086%	0.0018%
C_4H_{10}	0.00822%	0.017%
N_2	76.20%	74.10%
OH	0.26%	0.13%
H	0.26%	0.13%

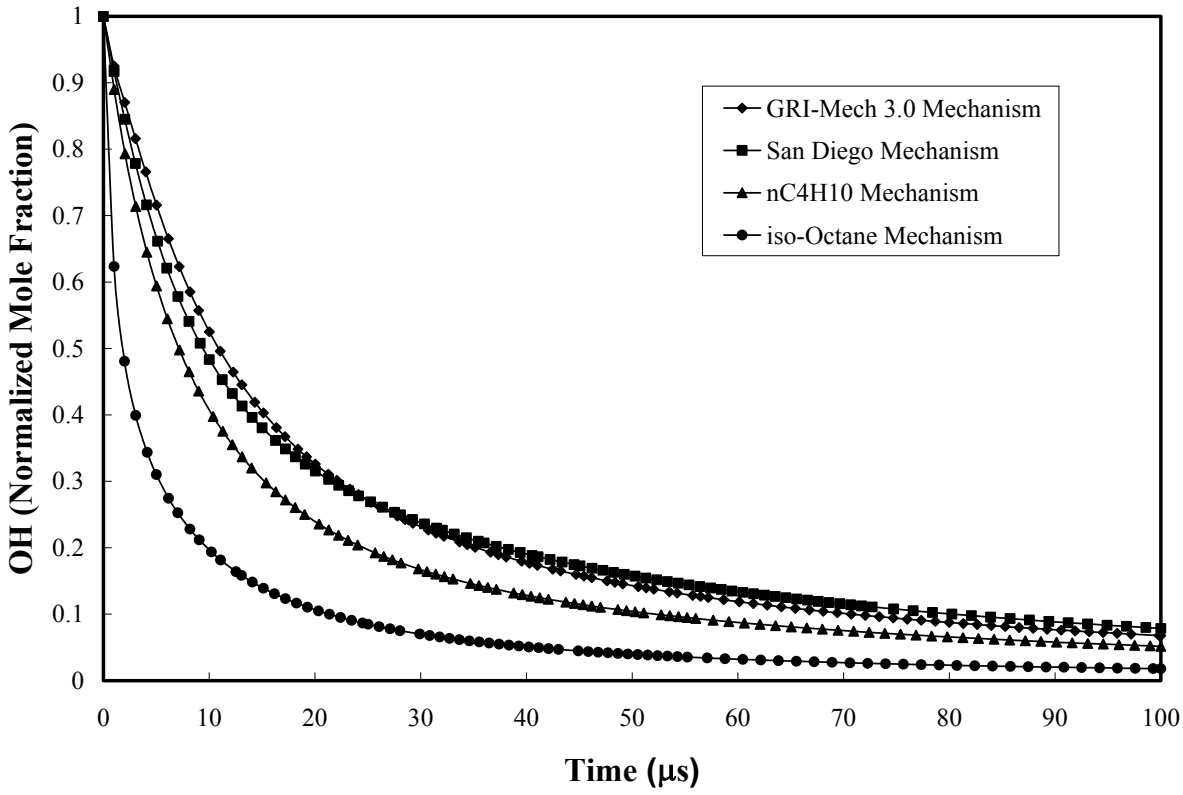

Fig. 6-3. OH Lifetime (no supplemental oxygen in product composition). (M = 5, T = 314 K, P = 18 kPa)

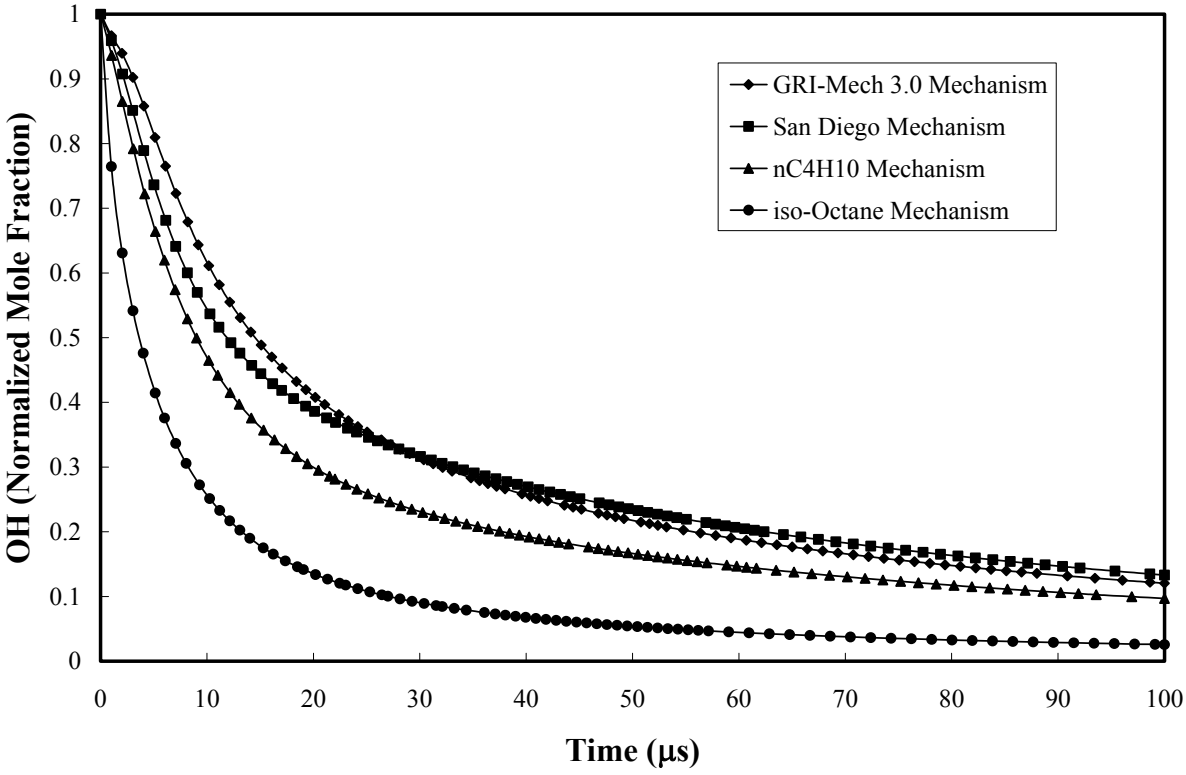

Fig. 6-4. OH Lifetime (supplemental oxygen in product composition). (M = 5, T = 314 K, P = 18 kPa)

even more limited room to transmit the laser beams with optics to such a large space, an alternative to bulky optical tables, mounts, and lenses has been proposed. Fiber optics can be used to transmit beams in an easily maneuverable framework. A set of UV fiber optics have been purchased, and tests will be conducted at Vanderbilt to demonstrate the ability of these fibers to transmit a single ArF beam to produce a cross of OH in the measurement zone. The line will be imaged to analyze the quality of the "write" beam using the UV fibers. Moreover, the scaling issues will be analyzed in person and in more detail at the APTU facility at AEDC.

CHAPTER VII

CONCLUSIONS

7.1 Summary

Non-intrusive measurements of velocity were obtained in a Mach 2 flow with a wall cavity flame holder at Wright-Patterson Air Force Base (WPAFB) with the use of hydroxyl tagging velocimetry. Under low- and high-backpressure conditions, instantaneous two-dimensional images were obtained in the freestream and in the cavity. The instantaneous planar measurements were analyzed to determine the mean and rms velocities in the streamwise direction. The rms values of the velocities in the freestream of the Mach 2 flow are low, consistent with the expected low turbulence values within the freestream and the OH line crossing-point displacement uncertainty equal to or better than 0.1 pixels. Under high-backpressure conditions the shocks in the cavity greatly modify the mean velocity profiles and greatly increase the rms velocity values. These measurements demonstrate the utility of the hydroxyl tagging method. Here, with only the addition of water to the flow, high-fidelity measurements of the velocity field of a high-speed flow above a recessed cavity are possible. Difficulties encountered with particle-based methods –especially in recirculation regions around high-speed core flows – are obviated with this approach.

Improvements were then made in the grid density by increasing the number of "write" lines to eleven on each grid optic producing a flow field with ~ 120 crossing points. HTV measurements were once again made at WPAFB from step-to-step in hopes

of producing a relevant supersonic data set for CFD modelers. This data analysis, using the MTV code developed at Michigan State, is still underway.

7.2 Conclusions

Hydroxyl Tagging Velocimetry has shown to be an excellent velocimetry tool for high speed, high temperature flow. With the success of the work conducted in supersonic flows at Wright-Patterson, the ultimate goal of applying this method to the APTU facility at AEDC is closer at hand. Many side tests have been undertaken to prepare for this endeavor, such as lifetime tests, vibration proof methodology, and particle scattering elimination. In addition, plans have been made to explore the scaling issues associated with a wind tunnel the size of APTU. Accessibility will play a major role in the application of this method to the facility.

Hypersonic flight vehicles and missile systems are definitely on the cutting edge of technology. From military to commercial use, the demand for this type of air breathing technology is on the rise. Hydroxyl tagging velocimetry is just one tool that can help aid in the pursuit of an operating hypersonic vehicle.

REFERENCES

Adrian, R. J. (1991), "Particle-imaging techniques for experimental fluid mechanics," *Annual Review of Fluid Mechanics*, **23**, 261-304.

Allen, M., S. Davis, W. Kessler, H. Legner, K. McManus, P. Mulhall, T. Parker, and D. Sonnenfroh (1994), "Velocity field imaging in supersonic reacting flows near atmospheric pressure," *AIAA Journal*, **32**, 1676-1682.

Barker P., A. Thomas, H. Rubinsztein-Dunlop, and P. Ljungberg (1995), "Velocity measurements by flow tagging employing laser enhanced ionisation and laser induced fluorescence," *Spectrochimica Acta,* **50B**, 1301-1310.

Ben-Yakar, A. and R. K. Hanson (2001), "Cavity flame-holders for ignition and flame stabilization in scramjets: an overview," *Journal of Propulsion and Power*, **17**, 869-877.

Boedeker, L. R. (1989), "Velocity measurement by H_2O photolysis and laser-induced fluorescence of OH," *Optics Letters*, **14**, 473-475.

Cohn, R. K. and M. M. Koochesfahani (2000), "The accuracy of remapping irregularly spaced velocity data onto a regular grid and the computation of vorticity," *Experiments in Fluids*, **29 (1)**, S61-S69.

Curran, H. J., P. Gaffuri, W. J. Pitz, and C. K. Westbrook (2002), "A Comprehensive Modeling Study of iso-Octane Oxidation," *Combustion and Flame*, **129**, 253-280.

Dam, N., R. J. H. Klein-Douwel, N. M. Sijtsema, and J. J. ter Meulen (2001), "Nitric oxide flow tagging in unseeded air," *Optics Letters*, **26**, 36-38.

Danehy, P. M., S. O'Byrne, A. F. P. Houwing, J. S. Fox, and D. R. Smith (2003), "Flow-tagging velocimetry for hypersonic flows using fluorescence of nitric oxide," *AIAA Journal*, **41**, 263-271.

Davidson, D. F., A. Y. Chang, M. D. DiRosa, and R. K. Hanson (1991), "Continuous wave laser absorption techniques for gas dynamic measurements in supersonic flows," *Applied Optics*, **30**, 2598-2608.

Drain, L. E. (1980), *The Laser Doppler Technique* (Wiley, New York).

Engel, V., G. Meijer, A. Bath, P. Andresen, and R. Schinke (1987), "The $C \rightarrow \tilde{A}$ Emission in Water: Theory and Experiment," *Journal of Chemical Physics*, **87**, 4310-4314.

Gendrich, C. P. and M. M. Koochesfahani (1996), "A spatial correlation technique for estimating velocity fields using molecular tagging velocimetry (MTV)," *Experiments in Fluids*, **22**, 67-77.

Gruber, M. R., J. M. Donbar, C. D. Carter, and K.-Y. Hsu (2004), "Mixing and combustion studies using cavity-based flameholders in a supersonic flow," *Journal of Propulsion and Power*, **20**, 769-778.

Gruber, M. R. and A. S. Nejad (1995), "New supersonic combustion research facility," *Journal of Propulsion and Power*, **11**, 1080-1083.

Hiller, B., R. A. Booman, C. Hassa, and R. K. Hanson (1984), "Velocity visualization in gas flows using laser-induced phosphorescence of biacetyl," *Review of Scientific Instruments*, **55**, 1964-1967.

Hjelmfelt, A. T., Jr., and L. F. Mockros (1966), "Motion of Discrete Particles in a Turbulent Fluid," *Applied Scientific Research*, **16**, 149-161.

Houwing, A. F. P., D. R. Smith, J. S. Fox, P. M. Danehy, and N. R. Mudford (2001), "Laminar boundary layer separation at a fin-body junction in a hypersonic flow," *Shock Waves*, **11**, 31-42.

Klavuhn, K. G., G. Gauba, and J. C. McDaniel (1994), "OH laser-induced fluorescence velocimetry technique for steady, high-speed, reacting flows," *Journal of Propulsion and Power*, **10,** 787-797.

Krüger, S. and G. Grünefeld (1999), "Stereoscopic flow-tagging velocimetry," *Applied Physics B*, **69**, 509-512.

Lempert, W. R., N. Jiang, S. Sethuram, and M. Samimy (2002), "Molecular tagging velocimetry measurements in supersonic microjets," *AIAA Journal*, **40**, 1065-1070.

Luque, J. and D. R. Crosley (1999), LIFbase: Database and Spectral Simulation, SRI International Report MP 99-009 http://www.sri.com/psd/lifbase.

Marinelli, W. J., W. J. Kessler, M. G. Allen, S. J. Davis, and S. Arepalli (1991), "Copper atom based measurements of velocity and turbulence in arc jet flows," *29th AIAA Aerospace Sciences Meeting*, Reno, NV, Jan. 7-10.

Marinov, N. M., W. J. Pitz, C. K. Westbrook, A. M. Vincitore, M. J. Castaldi, and S. M. Senkan (1998), "Aromatic and Polycyclic Aromatic Hydrocarbon Formation in a Laminar Premixed n-Butane Flame," *Combustion and Flame*, **114**, 192-213.

McDaniel, J. C., B. Hiller, and R. K. Hanson (1983), "Simultaneous multiple-point velocity measurements using laser-induced iodine fluorescence," *Optics Letters*, **8**, 51-53.

Miles, R. B. and W. R. Lempert (1997), "Quantitative flow visualization in unseeded flows," *Annual Review of Fluid Mechanics*, **29**, 285-326.

Nichols, R. H. (1985), "Calculation of Particle Dynamics Effects on Laser Velocimetry Data," *Wind Tunnel Seeding systems for Laser Velocimeters*, NASA CP2393, 1-11.

Noullez, A., G. Wallace, W. Lempert, R. B. Miles, and U. Frisch (1997), "Transverse velocity increments in turbulent flow using the RELIEF technique," *Journal of Fluid Mechanics*, **339**, 287-307.

Okabe, H. (1978), *Photochemistry of Small Molecules* (Wiley, New York).

Orlemann, C., C. Schulz, and J. Wolfrum (1999), "NO-flow tagging by photodissociation of NO_2. A new approach for measuring small-scale flow structures," *Chemical Physics Letters*, **307**, 15-20.

Paul, P. H., M. P. Lee, and R. K. Hanson (1989), "Molecular velocity imaging of supersonic flows using pulsed planar laser-induced fluorescence of NO," *Optics Letters*, **14,** 417-419.

Pitz, R. W., T. M. Brown, S. P. Nandula, P. A. Skaggs, P. A. DeBarber, M. S. Brown, and J. Segall (1996), "Unseeded velocity measurement by ozone tagging velocimetry," *Optics Letters*, **21**, pp. 755-757.

Pitz, R. W. and J. W. Daily (1983), "Combustion in a turbulent mixing layer formed at a rearward-facing step," *AIAA Journal*, **21**, 1565-1570.

Pitz, R. W., J. A. Wehrmeyer, L. A. Ribarov, D. A. Oguss, F. Batliwala, P. A. DeBarber, S. Deusch, and P. E. Dimotakis (2000), "Unseeded molecular flow tagging in cold and hot flows using ozone and hydroxyl tagging velocimetry," *Measurement Science and Technology*, **11**, 1259-1271.

Powell, E. S. (1983), "Combustion Performance of a Vitiated Air Heater for a Freejet Facility," *20th JANNAF Combustion Meeting*, Monterey, CA, Oct. 17-20.

Rasmussen, C. C., J. F. Driscoll, C. D. Carter, and K.-Y. Hsu (2005), "Characteristics of cavity-stabilized flames in a supersonic flow," *Journal of Propulsion and Power*, **21**, 765-768.

Ress, J. M., G. Laufer, and R. H. Krauss (1995), "Laser ion time-of-flight velocity measurements using N_2^+ tracers," *AIAA Journal*, **33,** 296-301.

Ribarov, L. A. (2002), "Nonintrusive Molecular Velocity Measurements in Air and Reacting Flows Using Hydroxyl Tagging Velocimetry," *Ph.D. dissertation*, Vanderbilt University, Nashville, Tennessee.

Ribarov, L. A., J. A. Wehrmeyer, F. Batliwala, R. W. Pitz, and P. A. DeBarber (1999), "Ozone tagging velocimetry using narrowband excimer lasers," *AIAA Journal*, **37**, 708-714.

Ribarov, L. A., J. A. Wehrmeyer, S. Hu, and R. W. Pitz (2004), "Multiline hydroxyl tagging velocimetry measurements in reacting and nonreacting experimental flows," *Experiments in Fluids*, **37**, 65-74.

Ribarov, L. A., J. A. Wehrmeyer, R. W. Pitz, and R. A. Yetter (2002), "Hydroxyl tagging velocimetry (HTV) in experimental air flows," *Applied Physics B*, **74**, pp. 175-183.

Rubinzstein-Dunlop, H., B. Littleton, P. Barker, P. Ljungberg, and Y. Malmsten (2001), "Ionic strontium fluorescence as a method for flow tagging velocimetry," *Experiments in Fluids*, **30**, 36-42.

Santoro, R. J., S. Pal, R. D. Woodward, and L. Schaaf (2001), "Rocket testing at university facilities," *39th AIAA Aerospace Sciences Meeting*, Reno, NV, Jan. 8-11.

Seasholtz, R. G., F. J. Zupanc, and S. J. Schneider (1992), "Spectrally resolved Rayleigh scattering diagnostic for hydrogen-oxygen rocket plume studies," *Journal of Propulsion and Power*, **8**, 935-942.

Sijtsema, N. M., N. J. Dam, R. J. H. Klein-Douwel, and J. J. ter Meulen (2002), "Air photolysis and recombination tracking: A new molecular tagging velocimetry scheme," *AIAA Journal*, **40**, 1061-1064.

Smith, G. P., D. M. Golden, M. Frenklach, N. W. Moriarty, B. Eiteneer, M. Goldenberg, C. T. Bowman, R. K. Hanson, S. Song, W. C. Gardiner Jr., V. V. Lissianski, and Z. Qin. Retrieved March 28, 2005, from www.me.berkeley.edu/gri_mech/ (GRI-Mech 3.0).

Stier, B. and M. M. Koochesfahani (1999), "Molecular tagging velocimetry (MTV) measurements in gas phase flows," *Experiments in Fluids*, **26**, 297-304.

University of California San Diego Center for Energy Research. Retrieved March 28, 2005, from http://maemail.ucsd.edu/combustion/cermech/olderversion/ (San Diego Mechanism 2003/08/30).

van der Laan, W. P. N., R. A. L. Tolboom, N. J. Dam, and J. J. ter Meulen (2003), "Molecular tagging velocimetry in the wake of an object in supersonic flow," *Experiments in Fluids*, **34**, pp. 531-533.

Wehrmeyer, J. A., L. A. Ribarov, D. A. Oguss, and R. W. Pitz (1999), "Flame flow tagging velocimetry with 193-nm H_2O photodissociation," *Applied Optics*, **38**, 6912-6917.

Zimmermann, M. and R. B. Miles (1980), "Hypersonic-helium-flow-field measurements with the resonant Doppler velocimeter," *Applied Physics Letters*, **37**, 885-887.